Chapter 6

Layered Pge Paleoproterozoic (LIP) Intrusions in the N-E Part of the Fennoscandian Shield — Isotope Nd-Sr and $^{3}He/^{4}He$ Data, Summarizing U-Pb Ages (on Baddeleyite and Zircon), Sm-Nd Data (on Rock-Forming and Sulphide Minerals), Duration and Mineralization

T. Bayanova, F. Mitrofanov, P. Serov, L. Nerovich,
N. Yekimova, E. Nitkina and I. Kamensky

Additional information is available at the end of the chapter

http://dx.doi.org/10.5772/58835

1. Introduction

There are about 20 Palaeoproterozoic layered mafic-ultramafic bodies in Finland, most of which occur in a roughly east–west-trending, 300 kmlong belt known as the Tornio-Na.ra.nka.vaara Belt (Alapieti et al. 1990; Vogel et al. 1998; Iljina & Hanski 2005). The belt (Fig. 1) extends for a few kilometres into Sweden (Tornio intrusion), and for several tens of kilometres into the Russian Karelia (Olanga complex). Together the intrusions make up the Southern, or Fenno-Karelian Belt, FKB (Mitrofanov et al. 1997).

In the NE of the province, the Northern, or Kola Belt (KB) strikes northwestwards for about 500 km (Fig. 1). It includes more than ten isolated layered mafic-ultramafic bodies that are mostly ore-bearing (Mitrofanov et al. 1997). The central part of the Kola Belt has been suggested to be part of a triple junction typical of intraplate rifting (Pirajno 2007) and is occupied by the Monchegorsk Layered Complex with a fairly complete range of ore types (Cr, Cu, Ni, Co, Ti, V, Pt, Pd, Rh). The western and eastern arms of the triple junction are composed of large anorthosite-troctolite (Main Ridge, Pyrshin, Kolvitsa) intrusions (Fig. 1). The most typical PGE-bearing layered pyroxenite-norite-gabbroanorthosite intrusions of the Kola Belt (e.g. Mt Generalskaya, Monchegorsk Layered Complex, Fedorovo-Pansky) are confined to boundaries between early Proterozoic rifts which were in-filled with volcano-sedimentary rocks overlying the Archaean basement (Schissel et al. 2002; Mitrofanov et al. 2005). In these cases, similar to

those in Finland, the intrusive rocks underwent relatively low-grade local metamorphism and preserve cumulus and intracumulus minerals.

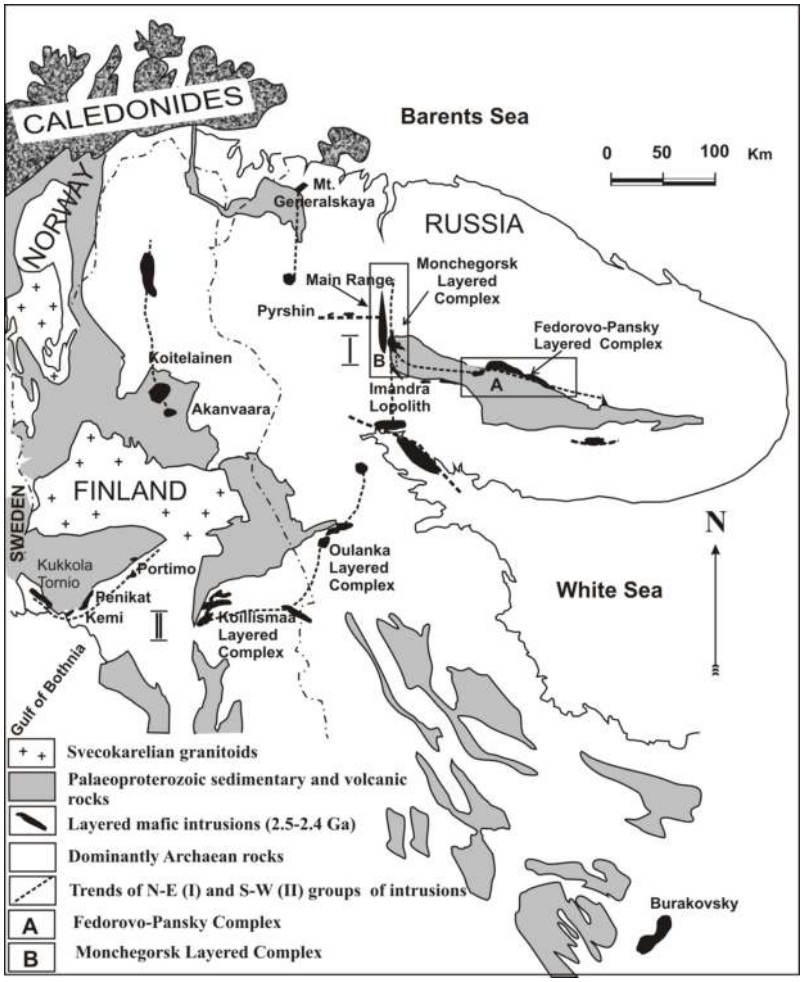

Figure 1. Generalized geological map of the northeastern part of the Baltic Shield and the location of Paleoproterozoic mafic layered intrusions (Mitrofanov et al., 2005).

Convincing arguments in support of the mantle plume hypothesis, either as 'shallow plumes' (from c. 670 km) or 'deep plumes' (from the core – mantle boundary) have been put forward for relatively young well-preserved Palaeozoic and recent large igneous provinces (LIPs) (Coffin & Eldhom 1994; Heaman 1997; Ernst & Buchan 2003; French et al. 2008). Voluminous magmatism is considered to be related to mantle plumes that occurred throughout the Precambrian (Condie 2001; Pirajno 2007). The best records of a plume source are Cu, PGE, Ti,

V and Fe. All the above-mentioned rock types, metals, host rift-associated volcanic rocks and mafic dykes are found in the relatively recently described East Scandinavian Palaeoproterozoic Large Igneous Province (LIP) (Iljina & Hanski 2005) with a total area of more than 200 000 km2 (Fig. 1). In Finland, these geological complexes have been widely studied (Alapieti et al. 1990; Huhma et al. 1990; Vogel et al. 1998; Hanski et al. 2001) and the data were suμmarized by Iljina & Hanski (2005). Only a few publications on similar Russian complexes of the Baltic Shield have been written or translated into English (Papunen & Gorbunov et al. 1985; Balashov et al. 1993; Bayanova & Balashov 1995; Bayanova 2009; Amelin et al. 1995; Sharkov et al. 1995; Mitrofanov et al. 1997; Mitrofanov & Bayanova 1999; Chashchin et al. 2002; Schissel et al. 2002; Mitrofanov et al. 2002, 2005).

This chapter presents a brief geological description of the Russian mafic-ultramafic intrusions of the Baltic Shield and associated mineralization. It focuses on new U–Pb (TIMS) and Sm–Nd geochronological data which constrain timing of magmatic pulses and the duration of the emplacement of Cr, Cu, Ni, Ti and PGE-bearing layered intrusions of the Kola Belt. Nd, Sr and He-isotope data help define geodynamic models for a long-lived early Precambrian mantle source expressed either in a large mantle diapir or multiple plume processes for one of the earliest clearly identifiable old intraplate LIPs and its metallogeny.

2. The Monchepluton, intrusions of the main ridge (Monchetundra and Chunatundra) and adjacent intrusions — Monchegorsk layered complex

The Monchegorsk Layered Complex (Fig. 2) has long been the subject of detailed investigation due to the exploitation of rich Cu–Ni ores of the Monchepluton (Papunen & Gorbunov 1985; Chashshin et al. 2002; Smolkin et al. 2004). The complex is located at a triple junction (Fig. 2) where weakly metamorphosed early Proterozoic rift-related rocks and deep-seated Archaean rocks metamorphosed at granulite to amphibo1ite facies become contiguous at the modem erosion level. The Monchepluton is an S-shaped body with an area of c. 65 km^2. It consists of two parts which probably represent independent magma chambers.

The northwestern and central parts of the Monchepluton (NKT: Mts Nittis, Kumuzhya and Travyanaya and Mt Sopcha) are mainly composed of non-metamorphosed ultramafic rocks, which from bottom-up are represented by a 10–100 mthick basal zone of quartz-bearing norite and gabbronorite, arzburgite (100–200 m), alternating harzburgite and orthopyroxenite (250–400 m), orthopyroxenite (300–700 m) with chromitite lenses (Mt Kumuzhya) and 1–5 m-thick Cu–Nibearing dunite-harzburgite layers (Mt Sopcha, '330 horizon'). The total thickness of the NKT intrusion expands southwards from 200–1000 m and culminates at Mt Sopcha (1600 m).

The southeastern part of the Monchepluton (NPV: Mts Nyud, Poaz and Vurechuaivench) consists mainly of 100–600 m-thick mafic rocks: basal quartz-bearing gabbronorite and norite (up to 50 m), melanocratic norite with lenses of olivinebearing harzburgite and norite, ore-bearing 'critical horizon' with xenoliths, olivine-free mesocratic and leucocratic norite and gabbronorite, gabbronorite, leucogabbro, anorthosite with PGE mineralization (Mt Vurechuaivench).

Both parts of the Monchepluton (NKT and NPV chambers) have a trough-like shape with a nearhorizontal floor and flanks dipping southwestwards at an angle of 20–40°. The complex is underlain by the Archaean gneiss and migmatite, and overlain by the Sumi rocks of the Imandra-Varzuga rift (near Mt Vurechuaivench). The intrusive rocks of the Monchepluton are cut by veins of basic to intermediate pegmatites and diorite, and by dolerite and lamprophyre dykes.

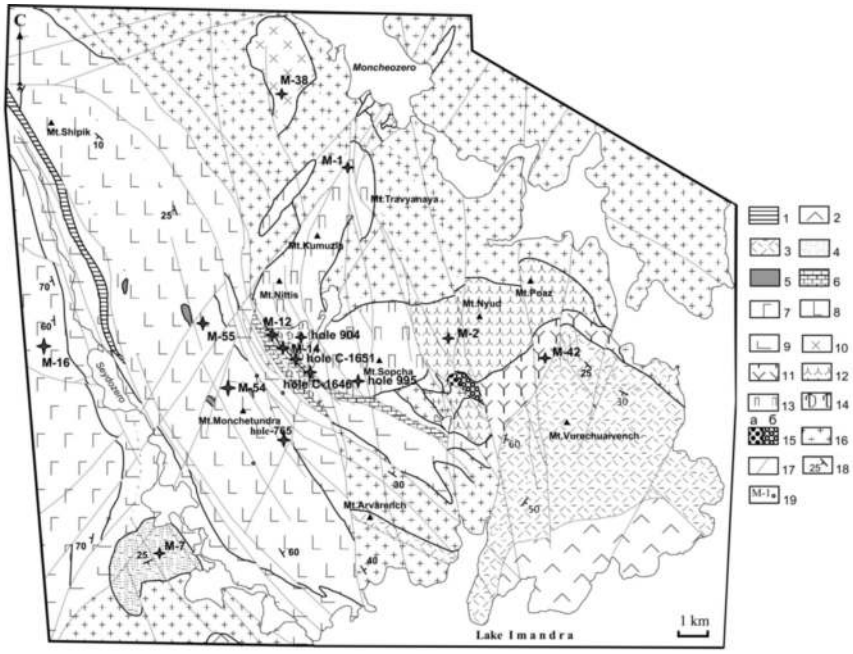

1- large gabbro-dolerite dykes, 2 –metagabbroid rock of the Umbarechka-Imandra complex, 3 – metasedimentary and metavolcanic rocks of the Imandra-Varzuga zone, 4 – lherzolite, websterite, orthopyroxenite and gabbronorite of the Ostrovsky intrusion , 5 - troktolite, 6 – large norite, orthopyroxenite and gabbro dykes, 7 – gabbro-anorthosite of the Chunatundra massif, 8 - metagabbro, gabbronorite and alternating orthopyroxenite and norite of the Monchetundra intrusion, 9 – cataclasis and recrystallization of gabbroid rocks of the Chuna and Monchetundra massifs, and that of Archean amphibolite, gneiss and diorite, 10 – norite, diorite and granophyric quartz diorite of the Yarva-Varaka massif, 11-14 Monchepluton: 11 - metagabbro, gabbronorite and anorthosite of the Vurechuaivench Foothills, 12 – olivine norite, norite, gabbronorite of the Nyud-Poaz, 13 - peridotite and pyroxenite of the NKT 14 – dunite of the Sopcheozero (Dunite) Block, 15 – diorite (a) and metagabbro (б) of the Xth anomaly, 16- Archaean basement rocks; 17 – faults, 18 – dip, 19 – numbered boreholes.

Figure 2. Geological map of the Monchegorsk layered complex (Smolkin et al. 2004).

The syngenetic disseminated Cu–Ni ore occurs in layers and is usually spatially confined to the layers of olivine-bearing rocks. The ore location is controlled by the primary structural elements of the intrusions. It also may be found in the upper and basal parts of the intrusions. The mineralization is related to the coarse-grained pegmatoid rocks. Occurrences of syngenetic and nest-disseminated ore with bedded, lens-shaped and stock-like forms are locally confined

to the parts of the intrusions where fine-grained and irregular-grained rocks, pegmatoids and rocks related to the intrusion ('critical horizon') are widely developed. The distribution of the two last-mentioned rock varieties may in some cases serve to reveal ore-controlling zones. Exploitable Cu–Ni–PGE deposits of veined epigenetic ores in the Monchepluton are confined to the systems of steeply dipping shear fractures trending NNE and dipping SSE, which trace the primary structural elements of the intrusion (geometry of intrusive blocks, primary jointing, etc.). The main ore-controlling elements in the occurrences of epigenetic stringer-disseminated ores are the zones of tectonic dislocations marked by schistose and blastomylonitized rocks. Most favourable for the concentration of injected stringer-disseminated ores are the places where the tectonic zones pass along the bend of the contact between rocks sharply different in physico-mechanical properties, for example between ultramafic rocks and Archaean granite-gneiss. The epigenetic sulphide Ni– Cu ores of the complex tend to occur in bodies with a mainly NE strike and SW plunge.

The rocks of the Monchepluton were dated earlier by U–Pb methods on zircons and baddeleyite at the Geological Institute KSC RAS (Bayanova 2004) and at the Royal Ontario Museum laboratory in Canada (Amelin et al. 1995) with a good convergence of results (see below). These ages fall in the range of 2507–2490 Ma and favour the correlation of the Monchepluton mafic-ultramafic layered series with the mafic layered series of the second intrusive phase of the Fedorovo-Pansky massif. In both intrusions, the main phase melts have produced Cu–Ni–PGE economic mineralization where base metals predominate, but the portion of platinum in the PGE disseminated occurrences is at least 20%. The ore bodies within the ultramafic rocks of the Monchepluton (Papunen & Gorbunov et al. 1985) are considerably richer than those of the Fedorov block deposit (Schissel et al. 2002). However, the deposits of the Monchegorsk region have already been mined out, while the Fedorovo-Pansky Complex is now being carefully investigated for future development.

Extensive areas of the Monchegorsk ore region are occupied by amphibolite-facies high-pressure garnet-bearing gabbronorite-anorthosite and anorthosite with numerous conformable and cutting veins of leucogabbro and pegmatoid rocks. These are the intrusions of the Main Ridge and Lapland-Kolvitsa granulite belts (Pyrchin, etc.) located within strongly metamorphosed country rocks.

The rocks of the intrusions are insufficiently studied by modern geological and petrological methods, but have been investigated by mining companies because of the presence of high PGE and V–Ti concentrations. The Monchetundra intrusion is separated from the Monchepluton by a thick (a few hundreds of metres) blastomylonite zone with a garnet-amphibole mineral association (Smolkin et al. 2004). Regional shear zones cut and transform the primary monolith-like shape of the intrusion composed of roughly layered leucocratic mafic rocks. This results in the lens-like morphology of the intrusions.

Available U–Pb isotope ages of these anorthosites fall in a wide time interval (Mitrofanov & Nerovich 2003; Bayanova 2004). The zircons derived from magmatic plagioclase yield an age varying from 2500–2460 Ma for different intrusions. A few generations of metamorphic zircons yield an age of multistage metamorphism that took place 2420, 1940 and 1900 Ma (Mitrofanov & Nerovich 2003).

3. Monchegorsk layered complex, isotope data

Ten samples of 50–120 kg were collected for U–Pb dating. Accessory baddeleyite and zircon were better preserved in drill core samples than in outcrops.

The oldest rocks studied are pegmatites of gabbronorite composition, which are associated with the ore-bearing sulphide veins from the basal zone of Mt Travyanaya and the 'critical horizon' (Mt Hyud, Terassa deposit). Two baddeleyite and three zircon populations were examined from these rocks. All the crystals were unaltered. Baddeleyite grains are up to 80 μm long and light brown in colour. Zircons are prismatic and isometric, up to 150 μm in size, and feature narrow igneous zoning and various hues of brown. U and Pb concentrations are high, which is typical of pegmatite. A U–Pb age obtained on the five zircon and baddeleyite populations is 2500±5 Ma, MSWD=1.7; the lower intersection of the discordia and the concordia is at 349±81 Ma, indicating Palaeozoic lead losses (Fig. 3A, Table 1). This age is comparable with that of 2493±7 Ma obtained for gabbronorite of Mt Nyud, and with a zircon age for the norite of Mt Travyanaya (Fig. 3B, Table 1). A U–Pb age on baddeleyite and zircon recently obtained for the coarse-grained gabbronorite of Mt Vurechuaivench foothills (now considered as a PGE-bearing reef) is 2497±21 Ma, being very similar to that for the Fedorovo-Pansky gabbronorite (Fig. 3C, Table 1).

To determine the age of the Sopcheozero chromite deposit located within the Dunite Block of the Monchepluton, cross-cutting dykes were analysed. The Dunite Block is composed of rocks poor in accessory minerals. The dykes are assumed to be associated with intrusive mafic rocks of the Monchepluton and are thought to have intruded the Dunite Block rocks before they had cooled. Thus the age of the dykes would constrain the minimum age limit of the Dunite Block and Sopcheozero deposit formation. For U–Pb dating, a sample was collected from Borehole 1586 at a depth of 63–125 m, from a coarse-grained gabbronorite dyke cutting the ultramafic rocks of the Dunite Block. Baddeleyite, two zircon populations and rutile were used for dating. Brown transparent plate-like baddeleyite grains of up to 70–80 μm in size are well preserved. Light-ink zircons of up to 150 μm in size have good outlines and thin zoning. The U–Pb age on zircon and baddeleyite is 2496±14 Ma, MSWD=0.011; the lower intersection of the discordia with the concordia is at 313±271 Ma (Fig. 3D, Table 1). The point for the rutile has a near concordant value of c. 1.84 Ga that reflects the time of its formation. A similar U–Pb age (2506±10 Ma) has also been obtained on zircon from a coarse-grained gabbronorite dyke from Borehole 1518 (Fig. 3E, Table 1). The gabbronorite dyke cuts the ultramafic rocks of the Dunite Block, therefore the Dunite Block must be older than the Monchepluton.

Small intrusions and dykes of the Monchegorsk Layered Complex were considered by most geologists to have the same age as the Monchepluton. In order to verify these relationships, diorite of the Yarva-Varaka intrusion was studied. Three zircon types and baddeleyite were selected from a sample of quartz diorite and granophyric hypersthenes diorite collected in the upper part of the Yarva-Varaka section. Stubby prismatic, pink-brown zircons of up to 150 μm in size were divided by their colour hues into three populations. In iμmersion view, they are multi-zoned. Baddeleyite grains and fragments are prismatic in habit, lightbrown coloured

and up to 80 μm in size. A U–Pb age obtained on four points is 2496±9 Ma, MSWD=0.93; the lower intersection is at zero, indicating recent lead losses (Fig. 3F, Table 1).

The Ostrovsky intrusion also belongs to the series of small mafic-ultramafic intrusions of the Monchegorsk Layered Complex. It was considered to correlate in age with the Monchepluton and was interesting as a target for Cu–Ni prospecting. A sample for U–Pb dating was taken from mafic pegmatite veins in the middle part of the upper gabbronorite zone (Mt Ostrovskaya). The pegmatite body is > 1 m-thick, up to 2 m long and has a complex morphology, with sinuous contacts with the coarsegrained slightly amphibolized host pigeonite gabbronorite. The sample is dominated by coarsegrained to pegmatoid gabbronorites with a poikilitic texture, made up mostly of calcic plagioclase and amphibolized clinopyroxene. The 60 kg sample produced two types of baddeleyite and two types of zircon. Baddeleyite grains of type 1 are up to 80 μm in size, with a deep-brown colour and flattened and tabular structure. Larger, up to 120 μm baddeleyite grains of type 2 were found within a fringe of metamict zircon and were exposed to aeroabrasion for 15 minutes in order to remove the metamict fringe. Zircons are prismatic, up to 125 μm in size, and are subdivided into light brown and brown varieties. Zircons show well-developed joints and thin zoning in iμmersion view. The U–Pb isochron age on two baddeleyite and two zircon points is 2445±11 Ma, MSWD=0.12 and the lower intersection of the discordia with the concordia is at 500±99 Ma (Fig. 3G, Table 1).

To establish age correlations between the gabbronorite of the Monchepluton and the anorthosite of the Main Ridge intrusion, rock samples of the Monchetundra and Chunatundra intrusions were studied.

The Monchetundra intrusion has a complex structure and an overview of geological and geochronological investigations is given by Smolkin et al. (2004). It includes the upper zone comprised mainly of amphibolized gabbronorite and gabbro-anorthosite, and the lower zone, which consists of gabbronorite, norite and plagiopyroxenite (drilled by the deep borehole M-1).

The middle part of the upper zone, which contains a prominent horizon of slightly-altered medium to coarse-grained gabbronorite with trachytoid texture, was sampled for U–Pb dating. The sample yielded three zircon types. Prismatic acicular crystals up to 200 μm in size and their brown fragments were divided into three types by colour. In iμmersion view, multi-zoning, mineral inclusions, strong jointing, corrosion of the surface and spotted uneven grain colour are observed. The U–Pb ages (Fig. 3H, Table 1) on zircon from trachytoid gabbronorite are 2505±6 Ma, MSWD=0.31 and 2501±8 Ma, (Fig. 3I, Table 1) MSWD=3 (Bayanova & Mitrofanov 2005).

A sample was also taken from the rocks of the differentiated series of the Chunatundra intrusion. Zircons from medium-grained leucogabbro with trachytoid texture were divided into five types. Four types are up to 150 μm isometric fragments of brown and pink colour, whereas the last fraction is represented by up to 120 μm twinned pinkishbrown zircons with adamantine lustre. The U–Pb isochron plotted on five points has the upper intersection with the concordia at 2467±7 Ma, MSWD=1.4 and the lower intersection is at zero (Fig. 3J, Table 1). This age is close to the age obtained on magmatic zircon from anorthosite of the Pyrshin

intrusion (Mitrofanov & Nerovich 2003) and on zircons from later anorthositic injections of the LLH (Fedorovo-Pansky Complex).

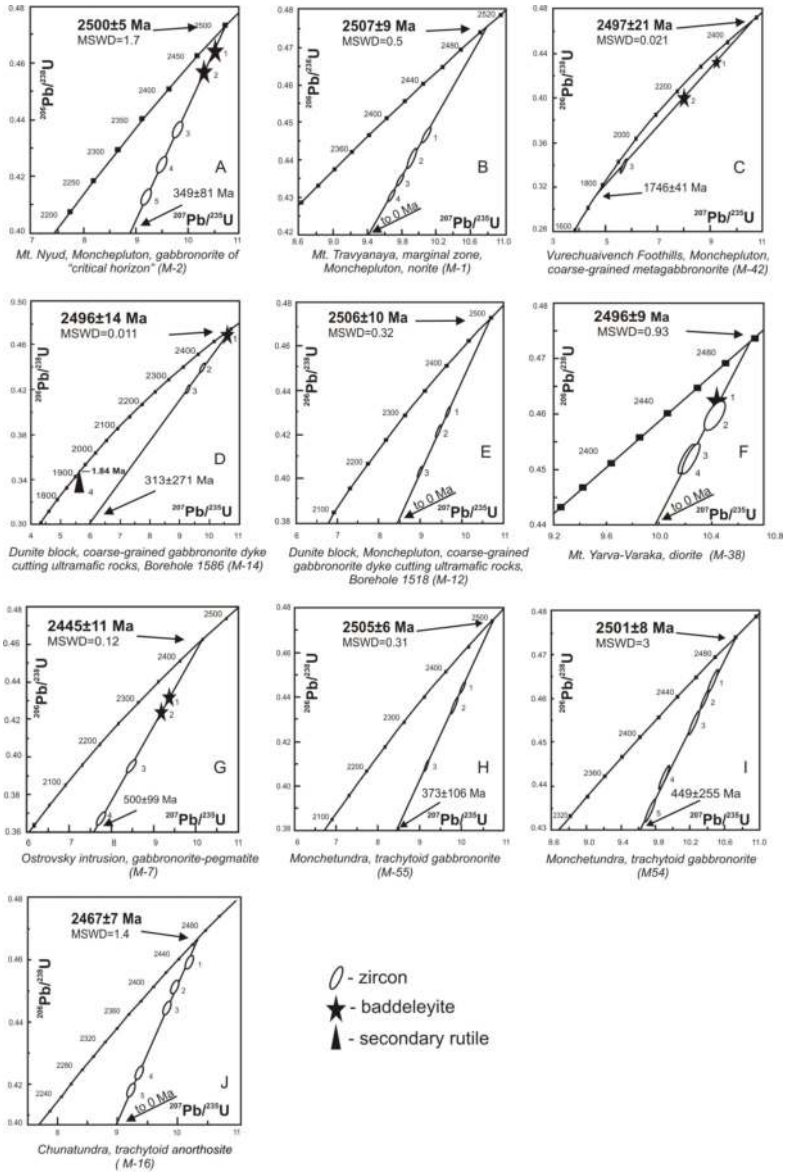

Figure 3. U–Pb concordia diagrams for zircon, baddeleyite and rutile from different rocks of the Monchegorsk Layered Complex.

http://dx.doi.org/10.5772/58835

Sample	No	Weight (mg)	Concentration (ppm)		Pb isotopic composition[1]			Isotopic ratios[2]		Age[2] (Ma)
			Pb	U	$^{206}Pb/^{204}Pb$	$^{206}Pb/^{207}Pb$	$^{206}Pb/^{208}Pb$	$^{207}Pb/^{235}U$	$^{206}Pb/^{238}U$	$^{207}Pb/^{206}Pb$
("critical horizon", Mt. Nyud Monchepluton, gabbronorite (M-2); from Bayanova, 2004)										
1 (bd)		0.70	93.1	198.8	9432	6.0586	103.8300	10.4643	0.4636	2495
2 (bd)		0.40	170.8	364.4	3589	5.9833	50.7070	10.3199	0.4574	2494
3		0.40	117.4	183.1	4590	6.0153	1.8703	9.8274	0.4359	2492
4		0.80	187.9	308.4	13664	6.1169	1.9750	9.4740	0.4227	2483
5		0.50	152.2	252.5	5300	6.0842	1.8994	9.2129	0.4125	2477
(marginal zone, Mt. Travyanaya Monchepluton, norite (M-1); from Smolkin et al., 2004)										
1		0.30	308.3	504.8	5778	6.0202	2.3805	10.0760	0.4458	2497
2		0.35	185.4	319.8	8358	6.0582	2.7721	9.9277	0.4402	2493
3		0.40	264.5	441.6	23762	6.1006	2.2929	9.7814	0.4342	2491
4		0.40	434.8	793.1	6273	6.0541	3.2613	9.7060	0.4314	2489
(Vurechuaivench Foothills Monchepluton, coarse-grained metagabbronorite (M-42); present study)										
1 *(bd)*		0.80	150.1	271.4	2982	6.3099	3.2054	9.23762	0.43446	2393
2 *(bd)*		0.65	65.1	122.6	2080	6.5863	2.7920	8.13574	0.40516	2295
3		0.75	137.4	288.5	911	6.4805	2.3018	5.75090	0.34208	2228
(Dunite block, Monchepluton, coarse-grained gabbronorite dyke cutting ultramafic rocks, hole 1586 (M-14); from Bayanova, 2004)										
1*(bd)*		0.50	5.3	10.3	1307	5.7748	12.4320	10.5720	0.4684	2494
2		0.80	358.7	309.2	13360	6.1029	0.5312	9.8622	0.4391	2486
3		0.60	321.8	362.1	3791	6.0407	0.7838	9.3919	0.4199	2479
4(ru)[3]		1.30	7.5	4.5	28	1.7085	0.8077	5.7139	0.3328	2022
(Dunite block, Monchepluton, coarse-grained gabbronorite dyke cutting ultramafic rocks, hole 518 (M-12); from Smolkin et al., 2004)										
1		0.45	221.4	409.6	2152	5.9237	3.5776	9.6682	0.4303	2487
2		0.30	321.7	542.6	11260	6.1264	2.2049	9.4976	0.4249	2478
3		0.50	164.9	302.4	1952	5.9508	2.5602	8.9806	0.4031	2472
(Mt. Yarva-Varaka, diorite (M-38); from Bayanova, 2004)										
1 *(bd)* 1		0.50	32.9	70.0	5615	6.0158	53.309	10.419	0.4608	2497
2		0.80	310.5	515.4	2587	5.9089	2.9118	10.420	0.4597	2501
3		1.40	151.8	262.7	4840	5.9895	3.1873	10.242	0.4519	2501

Sample No	Weight (mg)	Concentration (ppm)		Pb isotopic composition[1]			Isotopic ratios[2]		Age[2] (Ma)
		Pb	U	$^{206}Pb/^{204}Pb$	$^{206}Pb/^{207}Pb$	$^{206}Pb/^{208}Pb$	$^{207}Pb/^{235}U$	$^{206}Pb/^{238}U$	$^{207}Pb/^{206}Pb$
4	0.70	273.2	472.5	4590	5.9970	3.1828	10.217	0.4518	2497
(Ostrovsky intrusion, gabbronorite-pegmatite (M-7); from Bayanova, 2004)									
1 *(bd)*	0.45	28.6	63.9	1820	6.162	29.610	9.350	0.4311	2405
2 *(bd)*	0.55	36.3	83.7	3380	6.346	42.038	9.210	0.4248	2389
3	0.45	336.4	694.8	9420	6.378	3.797	8.471	0.3953	2407
4	0.35	89.1	187.6	3700	6.375	2.942	7.756	0.3667	2384
(Monchetundra, trachytoid gabbronorite (M-55); from Smolkin et al., 2004)									
1	0.50	110.9	172.9	8690	6.0591	1.9737	10.0171	0.444092	2493
2	0.35	37.7	61.0	1122	5.7260	2.2170	9.82794	0.436123	2492
3	0.25	168.3	277.7	6350	6.0914	1.8221	9.15540	0.409417	2479
4	0.30	122.6	213.5	6159	6.2294	1.9243	8.64155	0.395489	2439
(Monchetundra, trachytoid gabbronorite (M-54); from Smolkin et al., 2004)									
1	0.50	308.9	494.5	9172	6.0283	2.4881	10.47020	0.46359	2503
2	0.35	374.3	587.5	18868	6.0791	2.2742	10.40220	0.46050	2496
3	0.40	72.8	118.6	6833	6.0271	2.5023	10.25210	0.45405	2498
4	0.25	206.3	333.1	7831	6.0324	2.1148	9.90668	0.44177	2499
5	0.45	196.6	311.9	14844	6.1123	1.9269	9.74196	0.43412	2484
(Chunatundra, trachytoid anorthosite (M-16); from Bayanova, 2004)									
1	0.20	80.3	138.4	2710	6.020	3.404	10.216	0.4589	2471
2	2.05	122.83	214.1	4420	6.144	3.293	9.999	0.4527	2455
3	0.30	141.3	251.0	5140	6.137	3.291	9.831	0.4443	2461
4	0.60	92.7	169.4	7860	6.148	2.970	9.388	0.4228	2467
5	0.20	46.5	86.1	1090	5.805	3.242	9.262	0.4180	2463

[1]All ratios are corrected for blanks of 0.08 ng for Pb и 0.04 ng for U and for mass discrimination of 0.12±0.04%.

[2]Correction for common Pb was determined for the age according to Stacey and Kramers (1975).

[3]Corrected for isotope composition of light cogenetic plagioclase: $^{206}Pb/^{204}Pb$=14.041±0.005, $^{207}Pb/^{204}Pb$=14.581±0.007, $^{208}Pb/^{204}Pb$=35.58±0.02.

Table 1 U-Pb baddeleyite (bd), zircon and rutile (ru) isotope data from the Monchegorsk Layered Complex.

http://dx.doi.org/10.5772/58835

4. The Fedorovo-Pansky complex

The Fedorovo-Pansky Layered Complex (Fig. 4) outcrops over an area of > 400 km^2. It strikes northwestwards for > 60 km and dips southwestwards at an angle of 30–35°. The total rock sequence is about 3–4 km thick. Tectonic faults divide the complex into several blocks. The major blocks from west to east (Fig. 4) are known as the Fedorov, the Lastjavr, the Western Pansky and the Eastern Pansky (Mitrofanov et al. 2005). The Fedorovo-Pansky complex is bordered by the Archaean Keivy terrane and the Palaeoproterozoic Imandra-Varzuga rift. The rocks of the complex crop out close to the Archaean gneisses only in the northwestern extremities, but their contacts cannot be established due to poor exposure. In the north, the complex borders with the alkaline granites of the White Tundra intrusion. The alkaline granites were recently proved to be Archaean with a U–Pb zircon age of 2654±15 Ma (Bayanova 2004; Zozulya et al. 2005). The contact of the Western Pansky Block with the Imandra-Varzuga volcanosedimentary sequence is mostly covered by Quaternary deposits. However, drilling and excavations in the south of Mt Kamennik reveal a strongly sheared and metamorphosed contact between the intrusion and overlying Palaeoproterozoic volcano-sedimentary rocks that we interpret to be tectonic in origin.

The Fedorovo-Pansky Complex comprises predominantly gabbronorites with varying proportions of mafic minerals and different structural features. From bottom up, the composite layered sequence is as follows:

- Marginal Zone (50–100 m) of plagioclase–amphibole schists with relicts of massive fine-grained norite and gabbronorite, which are referred to as chilled margin rocks;
- Taxitic Zone (30–300 m) that contains orebearing gabbronoritic matrix (2485 Ma, see below) and early xenoliths of plagioclasebearing pyroxenite and norite (2526–2516 Ma, see below). Syngenetic and magmatic ores are represented by Cu and Ni sulphides with Pt, Pd and Au, and Pt and Pd sulphides, bismuthotellurides and arsenides;
- Norite Zone (50–200 m) with cumulus interlayers of harzburgite and plagioclase-bearing pyroxenite that includes an intergranular injection Cu–Ni–PGE mineralization in the lower part. The rocks of the zone are enriched in chromium (up to 1000 ppm) and contain chromite that is also typical of the rocks of the Penikat and Kemi intrusions (Finland) derived from the earliest magma portion (Iljina & Hanski 2005). Basal Cu–Ni–PGE deposits of the Fedorov Block have been explored and prepared for licensing (Schissel et al. 2002; Mitrofanov et al. 2005).
- Main Gabbronorite Zone (c. 1000 m) that is a thickly layered 'stratified' rock series (Fig. 4) with a 40–80 m thinly layered lower horizon (LLH) at the upper part. The LLH consists of contrasting alteration of gabbronorite, norite, pyroxenite and interlayers of leucocratic gabbro and anorthosite. The LLH contains a reef-type PGE deposit poor in base-metal sulphides. The deposit is now being extensively explored (Mitrofanov et al. 2005). According to the field investigations (Latypov & Chistyakova 2000), the LLH anorthositic layers have been intruded later, as shown by cutting injection contacts. This is confirmed by a zircon U–Pb age for the anorthosite of 2470±9 Ma (see below).

- Upper Layered Horizon (ULH) between the Lower and Upper Gabbro Zones. The ULH consists of olivine-bearing troctolite, norite, gabbronorite and anorthosite (Fig. 4). It comprises several layers of rich PGE (Pd-Pt) ore poor in base-metal sulphides (Mitrofanov et al. 2005). The U–Pb age on zircon and baddeleyite of the ULH rocks of 2447±12 Ma (see below) is the youngest among those obtained for the rocks of the Fedorovo-Pansky Complex.

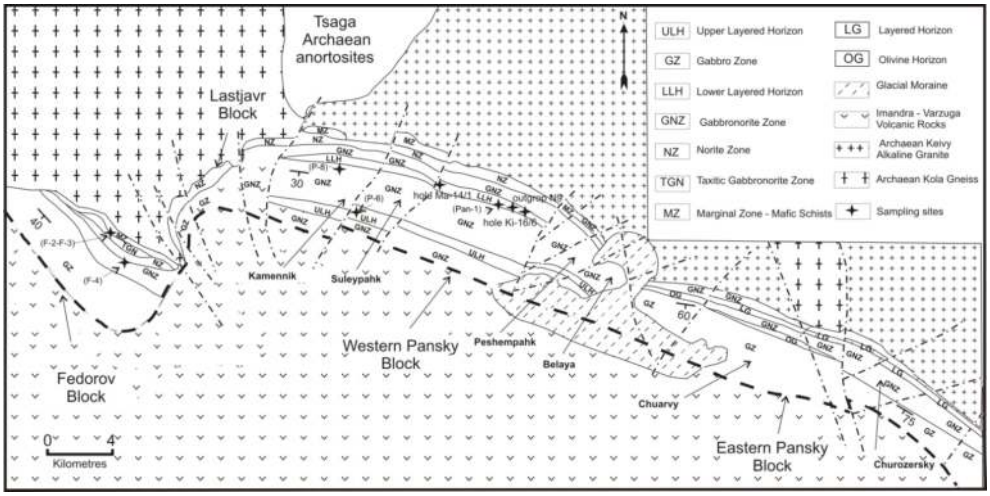

Figure 4. General geological map of the Fedorovo-Pansky Layered Complex (Mitrofanov et al. 2005).

5. Fedorovo-Pansky complex, isotope data

Several large samples were selected for the U–Pb dating of the Fedorovo-Pansky Complex.

A 60 kg sample of medium-and coarse-grained gabbronorite was collected from the Lower Layered Horizon in the Eastern Kievey area. The separated zircons are transparent with a vitreous lustre. All the grains were divided into three types: Pan-1–regular bipyramidal-prismatic crystals of up to 120 μm; Pan-2–fragments of prismatic crystals; Pan-3–pyramidal apices of crystals of 80–100 μm. In iμmersion view, all the zircons display a simple structure with fine zoning and cross jointing.

The discordia plotted on three points yields the upper intersection with the concordia and the U–Pb age at 2491±1.5 Ma, MSWD=0.05. The lower intersection of the discordia with the Concordia is at zero and reflects modern lead losses (Fig. 5A, Table 2). The same zircon sample was analysed in the Royal Ontario Museum laboratory in Canada; the obtained U–Pb zircon

age is 2501.5±1.7 Ma (Amelin et al. 1995) that is somewhat older than ours. The age obtained is interpreted as the time of crystallization of the main gabbronorite phase rock (Mitrofanov et al. 1997; Mitrofanov & Bayanova 1999).

Sm–Nd dating on ortho-and clinopyroxene, plagioclase and whole-rock minerals extracted from the same gabbronorite gave an age of 2487± 51 Ma, MSWD=1.5 (Balashov et al. 1993).

Three zircon populations of prismatic habit and light-yellow colour were separated from PGE-bearing gabbro-pegmatite (LLH). The zircons from sample P-8 are stubby prismatic crystals with sharp outlines, about 100 μm in size. The crystals show cross-cracks and apparent zoning in iμmersion view. The zircons from samples D-15 and D-18 are multi-zoned pinkish fragments of prismatic crystals with adamantine lustre and 80 and 100 μm in size. The U–Pb zircon age of 2470±9 Ma, MSWD=0.37 (Fig. 5A, Table 2) was obtained from three points: one concordant and two lying in the upper part of the isochron. The lower intersection of the discordia with the concordia (c. 300 Ma) indicates lead loss associated with the Palaeozoic tectonic activation of the eastern Baltic Shield and the development of the giant Khibina and Lovozero intrusions of nepheline syenites (Kramm et al. 1993). Zircons from the gabbro-pegmatite are found to have higher U and Pb concentrations than those from the gabbronorite.

Three zircon and two baddeleyite populations were separated from a sample collected from the Upper Layered Horizon in the Southern Suleypahk area. All the zircons from anorthosite are prismatic, light-pink-coloured with vitreous lustre. In iμmersion view, they are zoned and fractured. A population of bipyramidal-prismatic zircons (Pb-1) is made up of elongate (3:1) crystals. Sample Pb-2 contains zircons of round-ellipsoidal habit and sample Pb-3 contains transparent flattened crystal fragments of up to 0.75 μm in size.

The separated baddeleyite crystals (first recorded in the anorthosite) were subdivided into two varieties, deep-brown and brown. All the grains are fragments of transparent baddeleyite crystals of 50 μm in size, without selvages and inclusions.

A U–Pb isochron plotted from three zircons and two baddeleyites intersects the concordia with an age of 2447±12 Ma, MSWD=2.7 (Fig. 5B, Table 2). The lower intersection of the Discordia with the concordia records recent lead loss. The position of the baddeleyite points is near-concordant, while zircon points (Sample P6-1) are above the concordia due to uranium loss. This age (2447±12 Ma) is considered to constrain the origin of latephase anorthosite because, as shown by Heaman & LeCheminant (1993), baddeleyite is coμmonly generated in residual melts.

The U–Pb zircon age of the early barren orthopyroxenite from the Fedorov Block, 2526±6 Ma, is believed to be the time of emplacement (Fig. 5C, Table 2). The U–Pb age of 2516±7 Ma (Fig. 5D, Table 2), obtained from zircon from barren olivine gabbro, is interpreted as the time of crystallization. The last Cu–Ni–PGE-bearing taxitic gabbronorite from the Fedorov Block (Fig. 5E, Table 2) yielded a U–Pb zircon age of 2485±9 Ma (Nitkina 2006).

Ihe coeval Sm-Nd isotope ages have been oblained using rock-forming minerals from the same rork of the Fedorovo-Pansky massif (Fig. 6, Table 3).

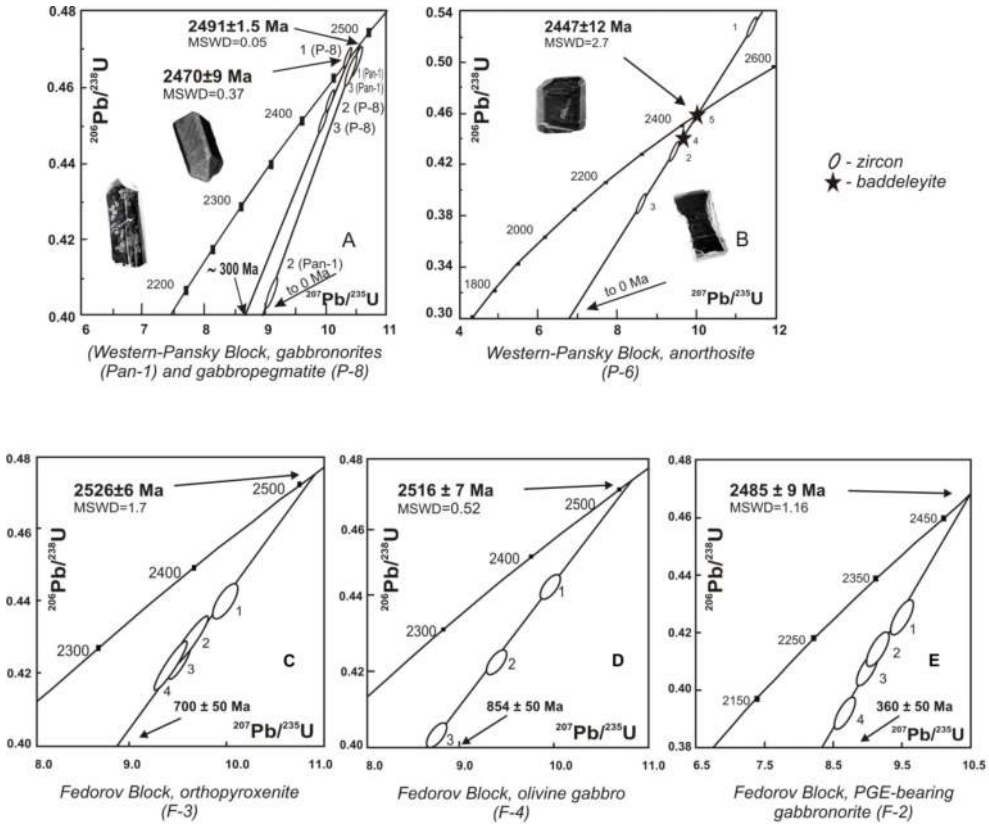

Figure 5. U–Pb concordia diagrams for the Western-Pansky (a, b) and Fedorov (c, d, e) Blocks of the Fedorovo-Pansky Complex.

SampleNo	Weight	Concentration		Pb isotopic composition[1]			Isotopic ratios[2]		Age[2]
	(mg)	(ppm)							(Ma)
		Pb	U	$^{206}Pb/^{204}Pb$	$^{206}Pb/^{207}Pb$	$^{206}Pb/^{208}Pb$	$^{207}Pb/^{235}U$	$^{206}Pb/^{238}U$	$^{207}Pb/^{206}Pb$
(Western-Pansky Block, gabbronorites (Pan-1); from Bayanova, 2004)									
1	3.30	95.0	144	11740	6.091	3.551	10.510	0.4666	2491
2	1.90	70.0	142	10300	6.100	4.220	9.135	0.4061	2489
3	1.60	84.0	144	6720	6.062	3.552	10.473	0.4650	2491

http://dx.doi.org/10.5772/58835

SampleNo	Weight	Concentration		Pb isotopic composition[1]			Isotopic ratios[2]		Age[2]
	(mg)	(ppm)							(Ma)
		Pb	U	$^{206}Pb/^{204}Pb$	$^{206}Pb/^{207}Pb$	$^{206}Pb/^{208}Pb$	$^{207}Pb/^{235}U$	$^{206}Pb/^{238}U$	$^{207}Pb/^{206}Pb$
(Western-Pansky Block, gabbropegmatite (P-8); from Balashov et al., 1993)									
1	5.90	95.0	158	3240	5.991	3.081	10.435	0.4681	2471
2	7.30	181.0	287	8870	6.161	2.260	10.092	0.4554	2465
3	1.25	125.0	200	3400	6.012	2.312	10.082	0.4532	2468
(Western-Pansky Block, anorthosite (P-6); from Bayanova, 2004)									
1	0.75	218.0	322	5740	6.230	3.263	11.682	0.5352	2438
2	0.10	743.0	1331	3960	6.191	3.151	9.588	0.4393	2438
3	0.20	286.0	577	2980	6.021	3.192	8.643	0.3874	2474
4 (bd)	1.00	176.0	396	14780	6.290	63.610	9.548	0.4380	2435
5 *(bd)*	0.26	259.0	560	3360	6.132	54.950	9.956	0.4533	2443
(Fedorov Block, orthopyroxenite (F-3); from Nitkina, 2006)									
1	0.75	48.0	60.9	825	4.9191	1.3039	10.0461	0.44249	2504
2	0.80	374.0	598.6	4588	6.0459	1.9650	9.6782	0.43153	2484
3	0.85	410.2	630.2	4521	6.0281	1.6592	9.5667	0.42539	2488
4	1.00	271.0	373.1	2552	5.9916	1.2393	9.4700	0.42406	2476
(Fedorov Block, olivine gabbro (F-4); from Nitkina, 2006)									
1	1.80	725.3	1322.8	14649	6.1121	3.8177	10.0132	0.44622	2484
2	2.00	731.3	1382.8	8781	6.1522	3.5517	9.4306	0.42454	2467
3	1.95	680.9	1374.0	7155	6.2645	3.6939	8.7401	0.40155	2433
(Fedorov block, PGE-bearing gabbronorite (F-2); from Nitkina, 2006)									
1	0.30	498.0	833.4	2081	5.9502	2.2111	9.49201	0.42493	2477
2	0.65	513.8	932.2	5274	6.1519	2.6371	9.1373	0.41378	2458
3	0.55	583.2	999.3	3194	6.1132	2.0528	8.9869	0.40832	2452
4	0.80	622.5	1134.5	4114	6.1161	2.1914	8.6638	0.39165	2460

[1]All ratios are corrected for blanks of 0.1 ng for Pb and 0.04 ng for U and for mass discrimination of 0.17 ± 0.05%.

[2]Correction for common Pb was determined for the age according to Stacey and Kramers (1975).

Table 2 U-Pb baddeleyite (bd) and zircon isotope data from the Western-Pansky and Fedorov Blocks of the Fedorovo-Pansky Complex.

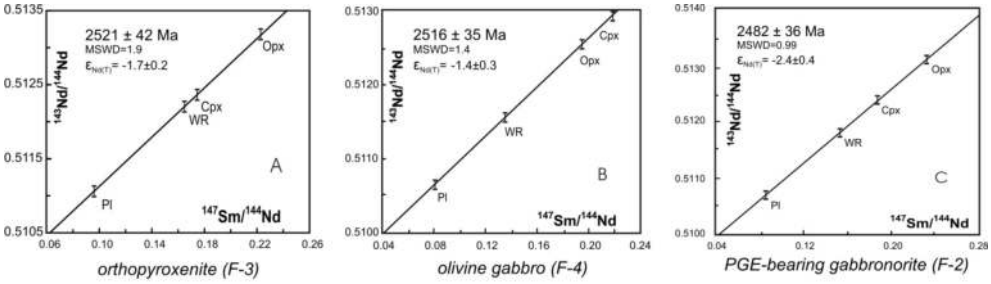

Figure 6. Mineral Sm–Nd isochrons for rocks and rock-forming minerals of the Fedorov Block of the Fedorovo-Pansky Complex.

Sample No	Concentration (ppm)		Isotopic ratios		T_{DM} (Ga)	Sm-Nd (Ma)	$\varepsilon_{Nd\ (2.5Ga)}$
	Sm	Nd	$^{147}Sm/^{144}Nd$	$^{143}Nd/^{144}Nd$			
orthopyroxenite (F-3)							
WR	0.32	1.17	0.1648	0.512196±12	3.05	2521±42	-1.73
Opx	0.12	0.38	0.2228	0.513182±16			
Cpx	2.21	7.67	0.1745	0.512349±17			
Pl	0.26	1.62	0.0960	0.511071±29			
olivine gabbro (F-4)							
WR	0.63	2.80	0.1357	0.5115488	2.94	2516±35	-1.53
Opx	0.23	0.72	0.1951	0.51255515			
Cpx	0.83	2.28	0.2187	0.51294716			
Pl	0.24	1.77	0.0815	0.51067714			
PGE-bearing gabbronorite (F-2)							
WR	0.42	1.66	0.1537	0.51180720	3.18	2482±36	-2.50
Pl	0.41	2.88	0.0865	0.51070914			
Cpx	1.78	5.73	0.1876	0.5123878			
Opx	0.13	0.33	0.2323	0.51308840			

Table 3 Sm-Nd isotope data on whole rock and mineral separates of the Fedorov Block of the Fedorovo-Pansky Complex.

6. Analytical U-Pb, Sm-Nd, Rb-Sr methods

U–Pb (TIMS) method with $^{208}Pb/^{235}U$ tracer. Following the method proposed by Krogh (1973), the samples were dissolved in strong (48%) hydrofluoric acid at a temperature of 205–210 °C over 1–10 days. In order to dissolve fluorides, the samples were reacted with 3.1 N HCl at a temperature of 130 °C for 8–10 hours. To determine the isotope composition of lead and concentrations of lead and uranium, the sample was divided into two aliquots in 3.1 N HCl, and a mixed $^{208}Pb/^{235}U$ tracer was added. Pb and U were separated on an AG 1 × 8, 200–400 mesh anion exchanger in Teflon columns. The laboratory blank for the whole analysis was <0.1–0.08 ng for Pb and 0.01– 0.04 ng for U. All isotopic determinations for zircon and baddeleyite were made on Finnigan MAT-262 and MI 1201-T mass spectrometers and the Pb isotopic composition was analysed on a secondary-ion multiplier on a Finnigan MAT-262 in ion counting mode. The measurements of the Pb isotopic composition are accurate to 0.025% (Finnigan MAT-262) and 0.15% (MI 1201-T) when calibrated against NBS SRM-981 and SRM-982 standards, respectively. The U and Pb concentrations were measured in single-filament mode with the addition of H_3PO_4 and silica gel using the method (Scharer & Gower 1988; Scharer et al. 1996). Pb and U concentrations were measured within the temperature ranges of 1350–1450 and 1450–1550 °C, respectively. All of the isotopic ratios were corrected for mass discrimination during the static processing of replicate analyses of the SRM-981 and SRM-982 standards (0.12±0.04% for the Finnigan MAT-262 and 0.17±0.05% per a.m.u.). The errors in the U–Pb ratios were calculated during the statistical treatment of replicate analyses of the IGFM-87 standard and were assumed equal to 0.5% for Finnigan MAT-262 and 0.7% for MI 1201-T. If the actual analytical errors were higher, they are reported in the table of isotopic data. Isochrons and sample points were calculated Squid and Isoplot programs (Ludwig 1991, 1999). The age values were calculated with the conventional decay constants for U (Steiger & Jager 1977), all errors are reported for a 2 sigma level. Corrections for coμmon Pb were made according to Stacey & Kramers (1975). Corrections were also made for the composition of Pb separated from syngenetic plagioclase or microcline if the admixture of coμmon Pb was >10% of the overall Pb concentration and the $^{206}Pb/^{204}Pb$ ratios were <1000.

$^{205}Pb/^{235}U$ tracer for single grains. U-Pb (TIMS) method with based U-Pb method for single grain accessory minerals using ion-exchange chromatography. Handpicked crystals are first treated in ultrasonic bath for cleaning in spirit or in acetone, and then in 7N nitric acid, heated for about 15 minutes on a warm rangette, and finally are three times flushed with recurrent purification water. Chemical mineral decomposition is performed in teflon bombs with adding 3 to 5 mcl of mixed $^{205}Pb/^{235}U$ tracer using T. Krogh method (1973) in concentrated nitric acid during 5 to 7 days at a temperature of 210°C. After complete decomposition, the column effluent is evaporated on a warm ragette, and then 10 drops of 6.2N chlorohydric acid are added. The sample is placed to the thermostat for 8 to 10 hours at a temperature of 140-150°C for homogenization. Lead and uranium are separated for isotope investigations using ion-exchange chromatography in columns with Dowex IX8 200-400 mesh resin. Lead is eluted with 10 drops of 6.2N chlorohydric acid when also one drop of 0.1N phosphoric acid is added, and the solution is evaporated on a ragette down to 3 mcl. Uranium is eluted separately from lead with 20 drops of water with one drop of 0.1N phosphoric acid added, and evaporated

on a ragetter down to 3 mcl. All chemical procedures are carried out in the ultraclean block with blank Pb and U contamination of ca. 1-3 pg, and ca. 10-15 pg respectively. The measurement of Pb and U isotope composition and concentrations is performed on Re bands at seven-channel mass-spectrometer Finnigan-MAT 262 (RPG), on collectors, with ^{204}Pb and ^{205}Pb measured at a temperature of 1350-1450°C in an ion counting mode using a multiplier or quadrupole RPG accessory. Silicagel is used as an emitter. U concentrations are detected at a temperature of 1450-1550°C using a collector and a multiplier in a mixed statically dynamic mode. When U concentrations are negligible, the multiplier or quadrupole RPQ accessory is applied in a dynamic mode. All the measured isotope ratios are adjusted for mass-discrimination obtained when studying parallel analyses of SRM-981 and SRM-982 standards to be 0.12±0.04%. The coordinates of points and isochrone parameters are calculated using programs by K. Ludwig (1991, 1999). Ages are calculated in accordance with the accepted values of uranium decay constants (Steiger and Jger, 1977), with errors being indicated on a 2b level. The J. Stacey & J. Kramers model (1975) is used to adjust numbers for the admixture of coμmon lead.

Isotope Sm/Nd method. In order to define concentrations of samarium and neodymium, the sample was mixed with a compound tracer ^{149}Sm/^{150}Nd prior to dissolution. It was then diluted with a mixture of HF+HNO_3 (or+$HClO_4$) in Teflon sample bottles at a temperature of 100 °C until complete dissolution. Further extraction of Sm and Nd was carried out using standard procedures with twostage ion-exchange and extraction-chromatographic separation using ion-exchange tar «Dowex» 50 × 8 in chromatographic columns employing 2.3 N and 4.5 N HCl as an eluent. The separated Sm and Nd fractions were transferred into nitrate form, whereupon the samples (preparations) were ready for mass-spectrometric analysis. Measurements of Nd-isotope composition and Sm and Nd concentrations by isotope dilution were performed using a multicollector mass-spectrometer in a Finnigan MAT 262 (RPQ) in a static mode using Re +Re and Ta+Re filament. The measured reproducibility for ten parallel analysis of Nd-isotope composition for the standard La Jolla=0.511833±6 was <0.0024% (2σ). The same reproducibility was obtained from 11 parallel analyses of the Japanese standard: Ji Nd1=0.512078±5. The error in ^{147}Sm/^{144}Nd ratios of 0.2% (2σ), the average of seven measures, was accepted for statistic calculations of Sm and Nd concentrations using the BCR standard. The blanks for laboratory contamination for Nd and Sm are 0.3 and 0.06 ng, respectively. Isochron parameters were developed from programs of Ludwig (1991, 1999). The reproducibility of measurements was ±0.2% (2σ) for Sm/Nd ratios and ±0.003% (2σ) for Nd-isotope analyses. All ^{147}Sm/^{144}Nd and ^{143}Nd/^{144}Nd ratios were normalized to ^{146}Nd/^{144}Nd=0.7219 and adjusted to ^{143}Nd/^{144}Nd. 0.511860 using the La Jolla Nd standard. The ε_{Nd} (T) values and model TDM ages were calculated using the currently accepted parameters of CHUR (Jacobsen & Wasserburg 1984): ^{143}Nd/^{144}Nd=0.512638 and ^{147}Sm/^{144}Nd=0.1967 and DM (Goldstein & Jacobsen 1988): ^{143}Nd/^{144}Nd=0.513151 and ^{147}Sm/^{144}Nd=0.2136.

Sm-Nd method for studying suphides. The chemical and analytical treatment of sulphide minerals (pyrite, pentlandite, chalcopyrite, etc.) for Sm-Nd study is performed following a modified technique (Yekimova 2011) as compared to the conventional one (Zhuravlyov et al. 1987). To decompose sulphides, a mineral weight (20 to 50 mg) is mixed with a ^{149}Sm/^{150}Nd

tracer solution, treated with aqua regia ($HCl+HNO_3$) until complete decomposition, and evaporated dry. Afterwards, this is transformed to chlorides through evaporating the sample in 4.5-6N HCl. After the fractional acid decomposition, the dry residue is dissolved in ~1ml 2.3N HCl, and total REEs are separated from the solution via cation-exchange chromatography. A stepwise elution method is applied to 2.3 and 4.5N HCl in a chromatographic column with cation-exchange resin Dowex 50x8 (200-400 mesh). The separated REE fraction is evaporated dry, dissolved in 0.1N HCl, and loaded to the second column with KEL-F solid ion-exchange resin HDEHP. The resin is used to separate Sm and Nd. The selected Sm and Nd fractions are evaporated to get prepared for further mass-spectrometric analysis. All the measurements of the Nd isotope composition and Sm and Nd concentrations using an isotope dilution technique were performed at a seven-channel solid-phase mass-spectrometer Finnigan-MAT 262 (RPQ) in a static double-band mode in collectors using Ta+Re filaments. Re filaments were used as ionizers, and the sample was applied to the Ta filament with a diluted the H_3PO_4 microdrop being deposited on beforehand. The reproducibility error for eleven Nd isotope composition determinations of La Jolla=0.511833±6 (2σ, N=11) has been within 0.0024% (2σ). The same error was obtained when measuring forty-four parallel analyses of a new Japanese standard, JNd_i1=0.512072±2 (2σ, N=44). The error in $^{147}Sm/^{144}Nd$ ratios is accepted for the static calculation of the Sm and Nd concentrations in BCR-1 to be 0.2 % (2σ), which is an average of seven measurements. The blank intralaboratory contamination in Nd and in Sm is 0.3 ng and 0.06 ng respectively. The measured Nd isotope rations were normalized per $^{148}Nd/^{144}Nd$=0.241570, and recalculated for $^{143}Nd/^{144}Nd$ in LaJolla=0.511860 afterwards. The isochron parameters were computed using K. Ludwig programs (Ludwig 1991, 1999). The decompositions constants are as per (Steiger 1977). The ε_{Nd} parameters for a one-stage model were calculated using [De Paolo 1981], and for a two-stage model using (Liew & Hofmann 1988).

Isotope Rb/Sr method. The samples and minerals were all treated with double distilled acids (HCl, HF and HNO_3) and H_2O distillate. A sample of 20–100 mg (depending on Rb and Sr contents) was dissolved with 4 ml of mixed HF and HNO_3 (5:1) in corked teflon sample bottles and left at a temperature of about 200 °C for one day. The solution was then divided into three aliquots in order to determine Rb and Sr isotope compositions and concentrations. These were measured by isotope dilution using separate ^{85}Rb and ^{84}Sr tracers. Rb and Sr extraction was performed by eluent chromatography with «Dowex» tar 50 × 8 (200–400 mesh); 1.5 N and 2.3 N HCl served as an eluent. Tar volumes in the columns were c. 7 and c. 4 sm^3. The separated Rb and Sr fractions were evaporated until dryness, followed by treatment with a few drops of HNO^3. Sr isotope compositions and Rb and Sr contents were measured by a MI-1201-T (Ukraine) mass spectrometer in the two-ribbon mode using Re filaments. The prepared samples were deposited on the ribbons in the form of nitrate. Sr isotope composition in all the measured samples was normalized to a value of 0.710235 recoμmended by NBS SRM-987. Errors on Sr isotope analysis (confidence interval of 95%) do not exceed 0.04%, and those of Rb–Sr ratio determination are of 1.5%. Blank laboratory contamination for Rb is 2.5 ng and for Sr 1.2 ng. The adopted Rb decay constant of Steiger & Jager (1977) was used for age calculations.

7. Geological setting and petrography features of Monchetundra massif

The Monchetundra intrusion belongs to Northern (Kola) belt and has a northwestwardly elongated oval shape with a total area of ca. 120 sq. km (Fig. 7). The length of the intrusion is ca. 30 km, and the width varies from 2 to 6 km. From east and southeast, the Monchetundra intrusion is separated from the Monchepluton intrusion by a thick mass of blastocataclasites and blastomilonites, and from west by the Viteguba-Seidozero fault. The shape of the intrusion is also compared with a lopolith. The intrusion generally plunges south-westwards, but in its central part the layering and trachytoid elements occur near-horizontally, dipping towards the axial part of the intrusion. The maximum vertical thickness of the Monchetundra intrusion cross-section exceeds 2 km (Fig. 7).

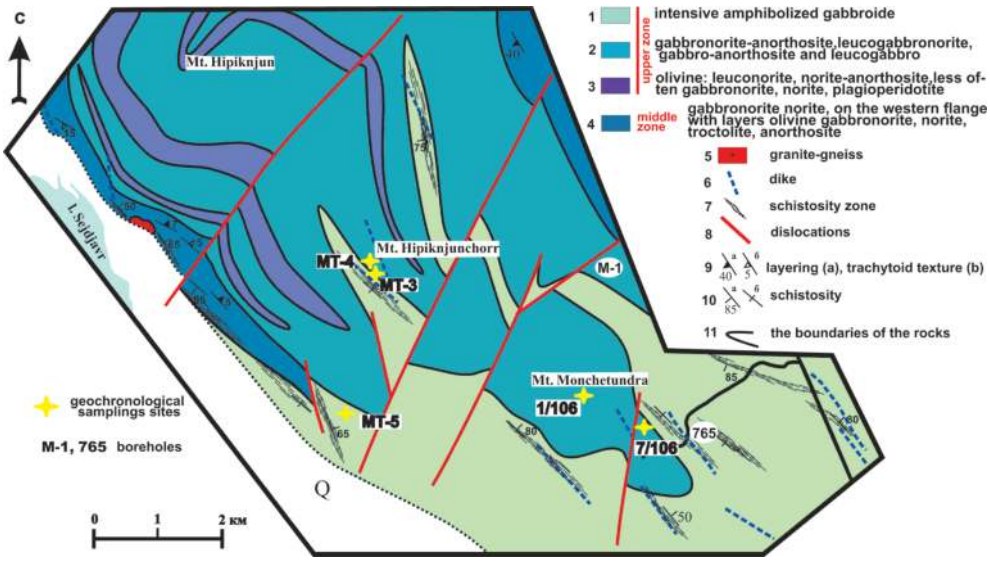

Figure 7. Schematic geological map of the central and southeastern parts of the Monchetundra intrusion (compiled by L.I. Nerovich on the materials of Central Kola Expedition OAO, Geological Institute KSC RAS with additions and amendments).

According to the results of the geological and petrographic study carried out on the principles of cumulative stratigraphy (Eules, Cawthorn, 1995; Irvine, 1982), the mafic and ultramafic rocks of the Monchetundra intrusion have been divided into three zones. The rock sequence of the lower zone (Fig. 8) varies from olivinite to leucocratic norite. The lower zone is dominated by norites with quite a wide distribution of pyroxenites and olivinites, which are coμmon in the south-eastern flank of the intrusion. Minor are harzburgites and gabbronorites. Orthopyroxene and olivine cumulates prevail in the cumulative stratigraphy of the lower zone. The rocks of the middle zone represent northwestwardly elongated strings at the exposed surface of the eastern and western flanks of the intrusion (Fig. 7) and compose a significant part of the

cross-section in the boreholes. The rock sequence of the middle zone ranges from troctolite and olivine gabbronorite to anorthosite. Contrast layering is more typical of the western flank of the intrusion. The lower zone is dominated by trachytoid medium-grained gabbronorite with plagioclase-pyroxene and minor plagioclase cumulates. The rocks of the upper zone make up the central part of the intrusion (Fig. 7).

8. Petrographical features rocks of the Monchetundra massif

In terms of composition, the rocks of the upper zone range from plagioperidotites to gabbronorite-anorthosites and gabbro-anorthosites. The contrast of the rocks increases northwestwards. Massive coarse-grained augite-pigeonite and augite-enstatite varieties of gabbronorite-anorthosites and leucogabbronorites, gabbro-anorthosite and leucogabbro prevail in the upper zone. The leucogabbro apparently represents an individual intrusive phase since there are xenoliths of leucocratic varieties of gabbronorites in the gabbro-anorthosites and leucogabbros of the upper and middle part of the Hipiknyunchorr Mt. slopes. The rocks of the upper zone correspond to plagioclase cumulates: poikilitic inclusions of plagioclase are typically observed in the pyroxenes and olivines.

Minor are plagioclase-pyroxene and plagioclase-olivine cumulates. Poikilitic inclusions of cumulus plagioclase in pyroxenes and olivines are found even in such melanocratic rocks as plagioperidotites of the upper zone. Thus, the lower zone of the Monchetundra intrusion consists of orthopyroxene and olivine cumulates, the middle zone of pyroxene-plagioclase and plagioclase cumulates, and the upper zone mainly of plagioclase cumulates.

Massive coarse-grained meso-leucocratic, mesocratic, and rarely melanocratic amphibole-plagioclase rocks are coμmon in the southeastern and southwestern parts of the Monchetundra intrusion (Fig. 7). These rocks are mainly thought to be altered varieties of leucogabbro, gabbro-anorthosite, and gabbro. Only relic clinopyroxene rarely shows well-preserved primary igneous features. The observed relic gabbro-ophytic and poikiloophytic structures indicate that the rocks are close to the leucogabbro and gabbro-anorthosite of the upper zone. However, secondary alteration of the rocks strongly hampers their investigation.

The internal structure of the Monchetundra intrusion displays significant lateral heterogeneity. The degree of differentiation tends to increase from the eastern flank of the intrusion southwards (for the lower zone) and westwards (for the middle and upper zones). This implies a possibility to find PGE mineralization not only at the junction of the Monchetundra and Monchepluton intrusions (eastern and southeastern flanks of the intrusion) that has mainly been investigated, but also in the rocks of the southwestern, western, and northwestern flanks of the intrusion.

The Monchetundra intrusion was earlier found to contain a level of noble metal mineralization confined to the norite and pyroxenite of the lower zone (Grokhovskaya et al., 2003; Smolkin et al., 2004). In 2005-2010, the exposed central and southeastern parts of the Monchetundra intrusion that are mainly composed of the upper zone rocks and of the middle zone rocks in

the eastern and western flanks, were sampled for a geochemical analysis. A geochemical sample of 2 kg was taken for analysis. The rocks were analyzed for PGE, Au and Ag using atomic absorption method at the Analytic Laboratory for noble metals of the Geological Institute KSC RAS. The resultant local anomalies of noble metals were confirmed by mineragraphic methods. The polished samples were studied with scanning electron microscope LEO-1450 at the Physical Analysis Laboratory of the Geological Institute KSC RAS.

The analysis of the geochemical data has shown that the local geochemical anomalies are mainly concentrated within the western slope of Mt. Monchetundra. The only exception is Mt. Hipiknyunchorr, where increased Pd content is observed along the whole intersection from east to west. On the whole, for the massive gabbroids of the upper zone, and for the dike and veins of the intrusion, oxide mineralization that is often accompanied by syngenetic chalcopyrite and epigenetic chalcosine-bornite-chalcopyrite masses, is more typical. It correlates with a slight increase in Pd and rarely Au content. A slight increase in Pd content is also registered in the chlorite-amphibole schists after gabbroids adjacent to the shear-fault displacement planes. No noble-metal minerals themselves have been found in the above-discussed cases. Higher concentrations of valuable components and noble-metal minerals are established in the trachytoid gabbronorite of the middle zone at the western flank of the intrusion. The mineralization traced for over 10 km has been clearly associated with the top of the middle zone in terms of structure and lithology. It points out the stratiform character of mineralization, similar of sulphides ores at Sudbury (Li, Naldrett, 1993).

9. Isotope — U-Pb data on zircon and baddeleyite from Monchetundra

The age of the lower zone has about established in Pentlandite gorge (the contact zone between Monchepluton and Monchetundra). The trachytoid gabbronorite of the middle zone emplaced – 2501±8 Ma and 2505±6 Ma (Bayanova et al., 2010). The gabbro-anorthosite of the upper zone was previously dated to have an age of 2453±4 Ma (Mitrofanov et al., 1993) that within error was confirmed by the investigations carried out within the present project (2456±5 Ma, Fig. 8A, Table 4). The ages of 2471±9 Ma and 2476±17 Ma obtained on baddeleyite that as a primary igneous mineral allows reliably establishing the time of crystallization corroborate the geological evidence of the earlier emplacement of the upper zone leucogabbronorite and gabbronorite-anorthosite based on the xenoliths found in the gabbro-anorthosite (Fig. 8B-C, Table 4). Thus, according to the U-Pb isotope study, two injection phases have been established for the upper zone of the Monchetundra intrusion: an earlier (2471±9 Ma, 2476±17 Ma) and a later (2456±5 Ma, 2453±4 Ma) one. The ages of 2420±5 Ma (Fig. 8D, Table 4) indicate the time of the earliest rock alterations and within error coincides with the alteration age of the other Early Proterozoic gabbro-anorthosite intrusions (Mitrofanov et al., 1993). A discordant age of 2521±8 Ma (Fig. 8E, Table 4), however, may indicate the presence of rocks of different age among strongly amphibolized gabbroids. The range of ages for the Monchetundra intrusion confirms its polychronous nature and long-term evolutional history, and is close to that for the Fedorovo-Pansky Complex (Balashov et al., 1993; Mitrofanov et al., 2005; Bayanova et al., 2009, 2010).

http://dx.doi.org/10.5772/58835

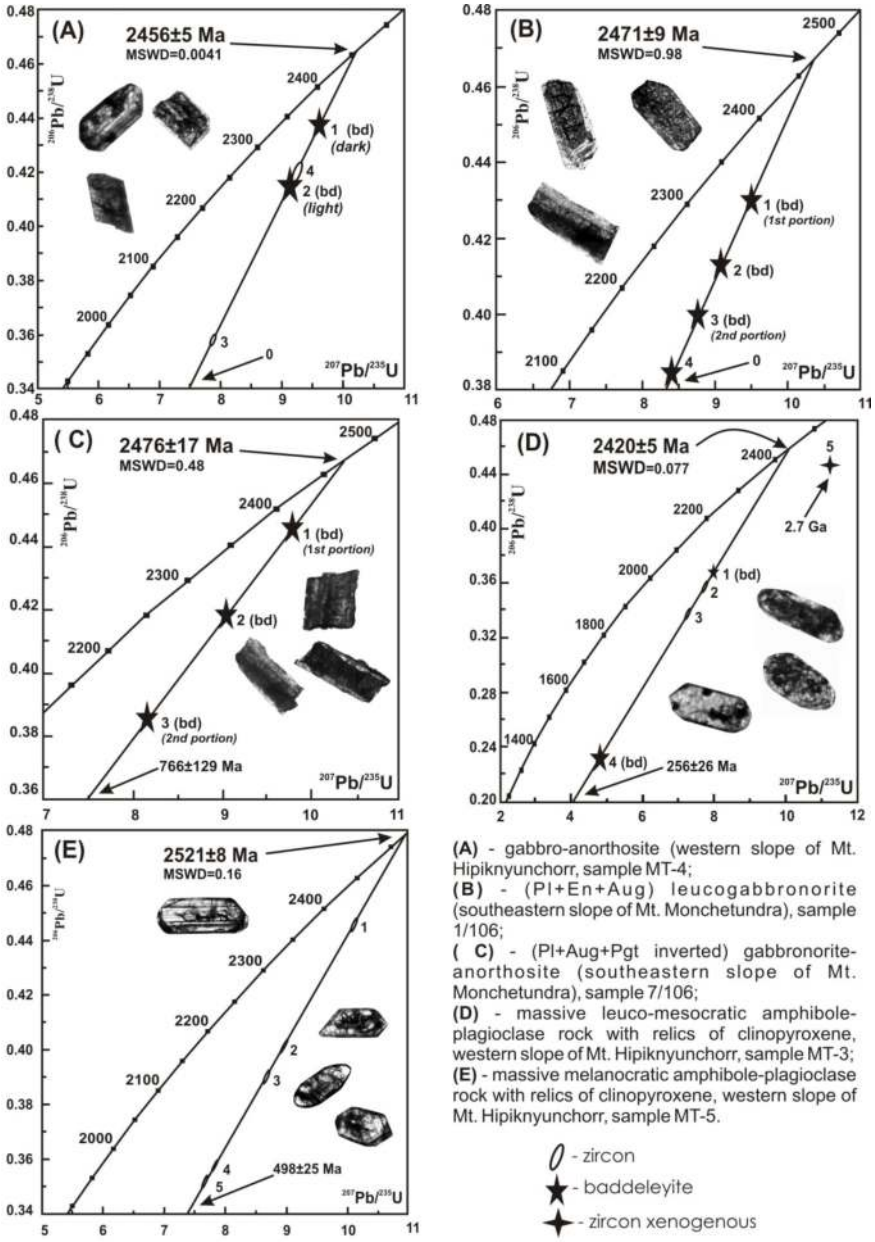

Figure 8. U–Pb concordia diagrams for zircon, baddeleyite and rutile from different rocks of the Monchegorsk Layered Complex.

No.	Weight of portion, Mg	Concentration, ppm		Pb isotope composition			Isotope ratios and age Ma**			Rho
		Pb	U	$^{206}Pb/^{204}Pb$	$^{206}Pb/^{207}Pb$	$^{206}Pb/^{208}Pb$	$^{207}Pb/^{235}U$	$^{206}Pb/^{238}U$	$^{207}Pb/^{206}Pb$	
Coarse-grained massive gabbro-anorthosite, slightly amphibolized, western slope of Mt. Khippiknyunchorr (MT-4)										
1	0.30 (bd)	62.2	138.3	3759	6.1220	35.850	9.64313	0.437144	2456	0.97
2	0.10 (bd)	45.5	107.9	4982	6.1556	48.241	9.12187	0.413717	2455	0.95
3	0.50 (zr)	348.4	634.6	7223	6.191	1.6275	7.88063	0.357735	2453	0.84
4	0.20 (zr)	216.8	420.0	562	5.7009	5.5664	9.06935	0.430759	2376	0.78
Medium-to-coarse-grained leucogabbronorite, southeastern slope of Mt. Monchetundra (1/106)										
1	0.50 (bd)	110.7	244.9	1478	5.9187	23.690	9.504470	0.429716	2460	0.94
2	0.35 (bd)	152.6	359.1	3510	6.1640	35.011	9.119096	0.413367	2441	0.95
3	0.50 (bd)	60.5	136.8	830	5.5615	13.663	8.820570	0.400447	2453	0.91
4	0.20 (bd)	98.0	246.4	1539	6.3461	24.580	8.368770	0.382377	2437	0.83
Medium-to-coarse-grained gabbronorite-anorthosite, southeastern slope of Mt. Monchetundra (7/106)										
1	0.25 (bd)	94.5	114.8	86	3.3003	2.2134	9.92226	0.450763	2500	0.70
2	0.20 (bd)	57.6	123.1	570	5.5602	11.459	9.08165	0.417879	2430	0.93
3	0.25 (bd)	30.1	67.9	557	5.6496	8.0718	8.19067	0.385383	2392	0.88
Medium-to-coarse-grained massive metamorphosed leucogabbro, western slope of Mt. Khippiknyunchorr (MT-3)										
1	0.35 (bd)	145.6	385.9	9943	6.6849	24.354	7.82654	0.368090	2326	0.94
2	0.40 (zr)	132.2	245.9	2892	6.4701	1.7904	7.68813	0.362228	2347	0.91
3	0.25 (zr)	296.5	590.4	10687	6.4780	1.7975	7.18160	0.340041	2382	0.94
4	0.20 (bd)	22.9	96.0	3075	6.4669	27.545	4.69641	0.232147	2351	0.86
5	0.15 (zr)	38.3	73.6	3640	5.2862	7.1653	11.6136	0.453251	2706	0.96
Medium-to-coarse-grained massive metamorphosed gabbro, western slope of Mt. Khippiknyunchorr (MT-5)										
1	0.20(zr)	442.9	674.4	11730	6.1317	1.3673	8.96466	0.401310	2477	0.95
2	0.20(zr)	110.7	187.1	4750	6.0548	1.6944	8.67071	0.389643	2482	0.85
3	0.30(zr)	717.3	1260.8	8770	6.1474	1.4718	7.83127	0.357492	2469	0.96
4	0.20(zr)	238.8	453.0	6557	6.2417	1.7384	7.67200	0.351541	2437	0.9

Notes: ratios corrected to the free-running contamination 0.08 ng for Pb and 0.04 ng for U and to mass-discrimination of 0.12±0.04 %. ** Correction to admixture of coμmon lead made for the age acc. to the model by Stacey and Kramers (Stacey, Kramers, 1975).

Table 4 Isotope U-Pb (ID-TIMS) data for baddeleyite (bd) and zircon (zr) from the rocks of the Monchetundra intrusion.

10. Pentlandite gorge (Monchetundra and Monchepluton): Isotope U-Pb age on single zircon and baddeleyite and Sm-Nd data on rock-forming and sulfides minerals from plagiopyroxenites

Pentlandite gorge is a very important part of Monchetundra massif so it is a contact place with Monchegorsk intrusions (Smolkin et al., 2004). From plagiopyroxenites of outcrops about 80 kg were separated accessory minerals-baddeleyite and zircon were very small sizes about 50-70 μm and about 1-2 mg. Baddeleyite grains are black and dark brown were separated by 2 types due to sizes. Zircon grains are brown and were a fragment of the crystals and subdivided onto 4 types on sizes. Isotope U-Pb dating presented in (Fig. 9A, Table 5) and all 6 points lie near the concordant with age 2502.3±5.9 Ma which reflect origin of plagiopyroxenite.

The final magmatic activity in Monchetundra massif connected with gabbro pegmatite rocks. About 50 kg of the rocks were taken for U-Pb single zircon dating. All zircon from separation procedures (Bayanova et al., 2009) were subdivided into 3 types due to colored. Grains of zircon are pink and have slightly rounded and corroded features with 100 μm in sizes. All zircon population in CL transmission are characterized by invisible zonetions and was separated into intensively of color on three types to U0Pb dating. Single zircon from gabbro-pegmatite on U-Pb isochron yielded 2445.1±1.7 Ma and reflect the age of crystallization of the rock (Fig. 9B, Table 5).

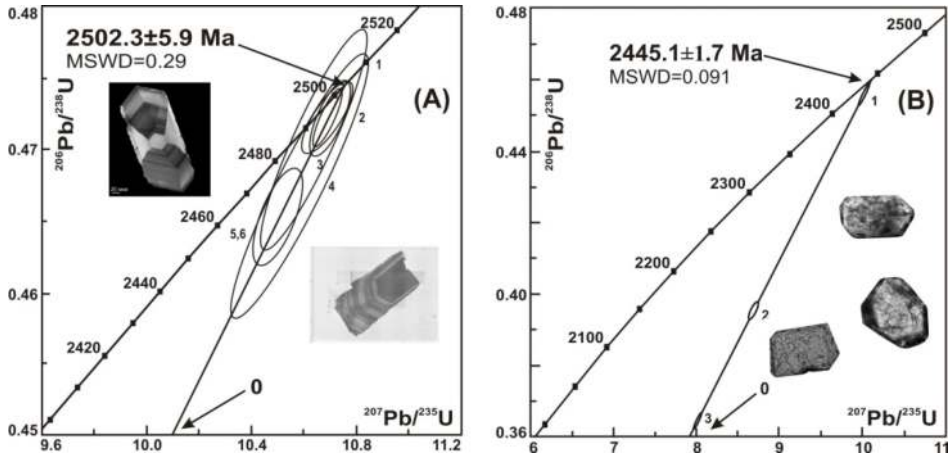

Figure 9. U-Pb concordia diagrams from Pentlandite gorge (Monchetundra massif) on: a-zircon (1-3, 6) and baddeleyite (4, 5) from plagiopyroxenite; b-zircon from gabbro-pegmatite.

From plagiopyroxenites of Pentlandite gorge were separated rock-forming minerals (Cpx and Opx, Pl) and sulfides (Po) to Sm-Nd dating. All 6 minerals yielded Sm-Nd isochron age with 2489±49 Ma (Fig. 10, Table 6) with positive ε_{Nd}=±1.2 and (model T_{DM} age – 3192 Ma). Two points of sulphides – mixture of sulfides and pyrrhotine together with rock-forming minerals have shown less error in Sm-Nd dating and possibilities using sulphides in dating of layered PGE intrusions (Yekimova et al., 2011). Value ε_{Nd}(T) is positive and considered as a result of depleted mantle reservoir (DM).

№	Weight mg	Concentration (ppm)			Isotopic composition[1)]			Isotopic ratios and age in Ma[2)]			% Dis
		Pb	U	$^{206}Pb/^{204}Pb$	$^{206}Pb/^{238}U$±2σ	$^{207}Pb/^{235}U$±2σ	$^{207}Pb/^{206}Pb$±2σ	$^{206}Pb/^{238}U$ ±2σ	$^{207}Pb/^{235}U$ ±2σ	$^{207}Pb/^{206}Pb$±2σ	
Plagiopyroxenite, zircon (1-3, 6) and baddeleyite (4, 5)											
1	0.099	25.45	38.49	1056.1	0.473±0.002	10.713±0.059	0.1644±0.0006	2496±11	2499±14	2501±8	0.2
2	0.093	25.46	30.49	975.1	0.472±0.002	10.687±0.059	0.1642±0.0006	2493±11	2496±14	2499±9	0.2
3	0.085	43.19	68.43	1084.9	0.472±0.002	10.684±0.049	0.1643±0.0004	2491±10	2496±11	2500±6	0.4
4	0.010	60.65	67.39	257.0	0.472±0.008	10.683±0.188	0.1640±0.0010	2493±40	2496±44	2499±18	0.2
5	0.010	60.07	69.55	414.1	0.467±0.007	10.588±0.178	0.1640±0.0010	2473±39	2488±42	2500±16	1.1
6	0.076	271.47	286.32	859.2	0.465±0.003	10.509±0.086	0.1638±0.0009	2463±15	2481±20	2495±14	1.3
Gabbro-pegmatite, zircon											
1	0.15	61.20	96.42	1709.4	0.4562±0.0033	10.003±0.074	0.1590±0.0003	2423±18	2435±18	2445±4	0.9
2	0.05	130.84	225.37	1594.9	0.3953±0.0029	8.678±0.080	0.1592±0.0009	2147±16	2304±21	2447±14	12.2
3	0.08	10.31	28.13	460.6	0.3650±0.0031	8.011±0.070	0.1599±0.0003	1361±12	1846±16	2447±5	44.4

[1)]The ratios are corrected for blanks of 1 pg for Pb and 10 pg for U and for mass discrimination 0.12 ± 0.04%.

[2)]Correction for common Pb was determined for the age according to Stacey and Kramers (1975).

Table 5 Isotope U-Pb data on zircon and baddeleyite from different rocks of Monchetundra massif.

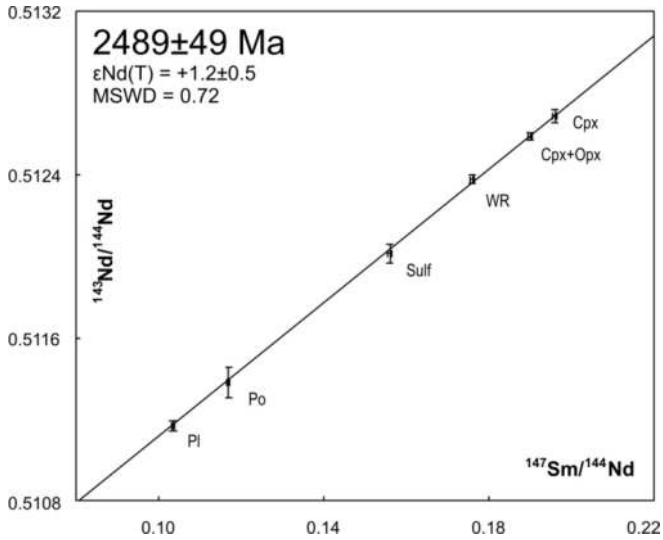

Figure 10. Isotope Sm-Nd mineral isochrone for rock-forming and sulphides minerals from plagiopyroxenites of Pentlandite gorge.

Sample	Concentration (ppm)		Isotope ratios		T_{DM} (Ga)	ε_{Nd} (2.5 Ga)
№	Sm	Nd	$^{147}Sm/^{144}Nd$	$^{143}Nd/^{144}Nd$		
P-1/109 WR	0.678	2.090	0.17617	0.512377±19	3192	±1.2
P-1/109 Po	0.018	0.095	0.11710	0.011381±59		
P-1/109 Sulf	0.032	0.123	0.15607	0.512015±43		
P-1/109 Cpx	1.048	3.230	0.19614	0.512687±33		
P-1/109 Opx±Cpx	1.095	3.374	0.19018	0.512586±16		
P-1/109 Pl	0.090	0.523	0.10363	0.511171±26		

Average standard values: N=11 (La Jolla:=0.5118336); N=100 (JNdi1:=0.51209815).

Table 6 Isotope Sm-Nd data on rock-forming and sulphides minerals from Pentlandite gorge.

11. Specific features of the isotope investigation of the intrusions

U-Pb (TIMS), Sm-Nd, and Rb-Sr methods have been applied in this work for different purposes.

The U-Pb concordia and isochron method has been used to define the age of the rocks. The values obtained on zircons and baddeleyites from the same sample usually lie at the isochron (Table 7), indicating a similar age of magma crystallization and subsequent transformations. Coordinates of baddeleyites are near the concordia line. The method however encounters the obstacle that mafic rocks contain very few zircon and baddeleyite grains. Samples of tens of kilograms yield only a few milligrams of these minerals.

The Sm-Nd system is not an accurate geochronometer (~2-5%). However, the Sm-Nd isochron method can allow the establishment of crystallization times for mafic rocks on major rock-forming minerals (orthopyroxene, clinopyroxene, and plagioclase). It is especially important for dating rocks with syngenetic ore minerals and sulphides. For example, this method has been used to determine for the first time the age (2426±38 Ma) of the early ore body in the Penikat Cu-Ni-PGE deposit of the Finland (Southern belt) that has economic importance (Yekimova et al., 2011).

Layered intrusions	**Age (Ma)**		**$\varepsilon_{Nd(T)}$ @ U/Pb age**
	U-Pb	Sm-Nd	
	Northern belt		
	Mt. Generalskaya		
gabbronorite	2496±10[1] (2505±1.6)[2]	2453±42[1]	-2.3
anorthosite	2446±10[1]		
	Monchepluton		
Mt. Travyanaya, norite	25079[15];		
Dunite block, gabbronorite dyke	2506±10[15]; 2496±14[15]		
Nyud Terrace, gabbronorite	25005[14]		
Nyud Terrace, gabbronorite	2493±7[1] (2504±1.5)[2]	2492±31[3]	-1.4
Vurechuaivench Foothills, metagabbronorite	2497±21[15]		
	Main Ridge		
Monchetundra, gabbro	246325[4]; 24534[5]		
Monchetundra, gabbronorite	2505±6[14]; 2501±8[14]		
Monchetundra, plagiopyroxenite	2502.3±5.9[17]; 2445.1±1.7[17]	2489±49[17]	+1.2
Chunatundra, anorthosite	2467±7[15]		
Ostrovsky intrusion, gabbronorite-pegmatite	244511[15]		
	Fedorovo-Pansky Complex		
orthopyroxenite	2526±6[12]	2521 ± 42[13]	-1.7
olivine gabbro	2516±7[12]	2516 ± 35[13]	-1.4
magnetite gabbro	2498±5[6]		

Layered intrusions	Age (Ma)		$\varepsilon_{Nd(T)}$ @ U/Pb age
	U-Pb	Sm-Nd	
gabbronorite	2491±1.5[7] (2501±1.7)[2]	2487±51[7]	-2.1
Cu-Ni PGE-bearing gabbronorite	2485±9[12]	2482 ± 36[13]	-2.4
PGE-gabbro-pegmatite	2470±9[7]		
PGE-anorthosite	2447±12[7]		
Imandra lopolith			
gabbronorite	2446±39[7](2441±1.6)[2]	2444±77[7]	-2.0
gabbro-diorite-pegmatite	24404[6]		
norite	24377[6]		
leucogabbro-anorthosite	243711[6]		
granophyre	243415[6]		
olivine gabbronorite (dyke)	23955[6]		
monzodiorite dyke	239821[6]		
Southern belt			
Kivakka, olivine gabbronorite	2445±2[7]	2439±29[8]	-1.2
Lukkulaisvaara, pyroxenite	2439±11[7] (2442±1.9)[2]	2388±59[8]	-2.4
Tsipringa, gabbro	2441±1.2[2]	2430±26[8]	-1.1
Burakovskaya intrusion, gabbronorite	2449±1.1[2]	2365±90[8]	-2.0
Kovdozero intrusion, pegmatoid gabbronorite	24369[6]		
Finnisn group			
Koitelainen	2433±8[9]	243749[11]	-2.0
Koilismaa	2436±5[10]		
Nyaryankavaara	2440±16[10]		
Penikat		2410±64[9]	-1.6
		2426±38[16]	-1.4
Akanvaara	24377[11]	242349[11]	-2.1

1. Bayanova et al., 1999	7. Balashov et al., 1993	13. Serov et al., 2007
2. Amelin et al., 1995	8. Amelin, Semenov, 1996	14. Bayanova & Mitrofanov, 2005
3. Tolstikhin et al., 1992	9. Huhma et al., 1990	15. Bayanova et al., 2009
4. Vrevsky, Levchenkov, 1992	10. Alapieti et al., 1990	16. Yekimova et al., 2011
5. Mitrofanov et al., 1993	11. Hanski et al., 2001	17. Present study (single U-Pb zircon-baddeleyite data)
6. Bayanova, 2006	12. Nitkina, 2006	

Table 7 Summary of U-Pb and Sm-Nd geochronology for layered intrusions located in the eastern Baltic Shield.

For the mafic-ultramafic intrusions of the Kola belt, the Sm-Nd ages overlap because of high errors, but are commonly close to the U-Pb (TIMS) data on zircon and baddeleyite.

Sample	**Concentration**		**Isotopic ratios**		**ε_{Nd}**	**T_{DM}**	**$^{87}Rb/^{86}Sr$**	**$^{87}Sr/^{86}Sr(\pm 2\sigma)$**
No	(ppm)				(2.5 Ga)	(Ga)		@2.5 Ga
	Sm	Nd	$^{147}Sm/^{144}Nd$	$^{143}Nd/^{144}Nd$ ($\pm 2\sigma$)				
Monchetundra								
MT-10, medium-grained pyroxenite	0.483	1.913	0.152689	0.51192533	-0.36	2.81	0.00495	0.7039±2
Mt. Generalskaya								
S-3464, gabbronorite	1.147	5.362	0.129320	0.511449±14	-2.30	2.91	0.00534	0.7042±2
Fedorovo-Pansky intrusion								
Pan-1, gabbronorite	0.762	3.293	0.139980	0.511669±7	-2.00	2.98	0.00135	0.7032±1
Pan-2, gabbronorite	0.423	1.662	0.153714	0.51180720	-2.50	3,18	0.00174	0.7029±2
F-4, olivine gabbro	0.629	2.801	0.135695	0.5115488	-1.53	2.94	0.00144	0.7029±2
F-3, orthopyroxenite	0.318	1.166	0.164803	0.512196±12	-1.73	3.05	0.00205	0.7033±2
Imandra lopolith								
6-57, gabbronorite	2.156	10.910	0.119130	0.511380±3	-2.00	2.88	0.00339	0.7046±3
Monchepluton								
M-1, quartz norite	1.750	8.040	0.131957	0.511493 ±3	-1.51	2.91	0.01053	0.7034±9
H-7, gabbronorite	0.920	4.150	0.134055	0.511537 ±4	-1.37	2.90	0.00227	0.7037±2

Table 8 Isotope Sm-Nd and Rb-Sr data for rocks of the layered Paleoproterozoic intrusions.

It is also important to stress that the Sm-Nd method provides valuable petrological and geochemical markers: $\varepsilon_{Nd}(T)$ and T_{DM}. The ε_{Nd} shows the degree of mantle magma source depletion, while T_{DM} indicates an approximate age of the mantle protolith (Faure, 1986).

The Rb-Sr whole rock and mineral isochron method is mostly valuable for dating unaltered felsic igneous rocks and metamorphic amphibolite-facies associations (Faure, 1986). In this work, in Rb-Sr isotope values for the rocks (Fig. 11, Table 8) are considered to have only a petrological implication. Together with specific trace elements (Cu, Ni, Ti, V, and LREE), ε_{Nd} (2.5 Ga), REE, ε_{Nd}-I_{Sr} (Fig. 11, Table 8), and $^{4}He/^{3}He$ (Table 9) data, the values of initial $^{87}Sr/^{86}Sr$ (I_{Sr}, 2.5 Ga) indicate an enriched mantle reservoir 2.5 billion years ago which is comparable with the modern EM-I (Hofmann, 1997).

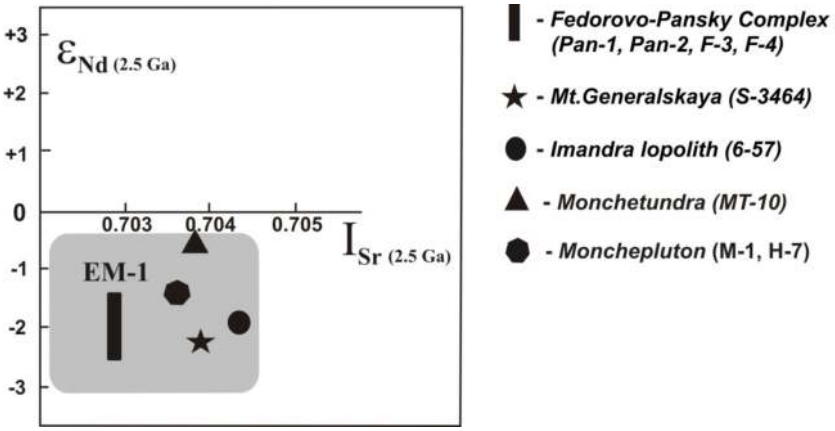

Figure 11. Isotope ε_{Nd}-I_{Sr} plot of rocks from the Northern (Kola) Belt layered intrusions. Grey colour in the diagram shows EM-1 reservoir plotted for the layered intrusions of the Kola Peninsula based on the Sm-Nd and Rb-Sr isotope data given in Table 8.

Hole No/sampling depth (m)	Rock, mineral	$^4He10^{-6}$ µcm^3/g	$^4He/^3He10^6$	Low Mantle contribution**%
Monchetundra				
hole, 765/905,9	Clinopyroxene	163.00	4.76	0.21
hole, 765/905,9	Orthopyroxene	21.00	4.76	0.21
hole, 765/985,3	Amphibole	97.00	4.76	0.21
hole, 765/985,3	Clinopyroxene	115.00	5.00	0.20
outcrop, MT-5	Gabbro	1.30	2.00	0.41
Fedorovo-Pansky intrusion				
hole, Ki-16/6	Amphibole	81.00	9.10	0.11
hole, Ma-14/1	Orthopyroxene	9.90	12.80	0.08
outcrop, No 9	Ilmenite	43.90	16.50	0.06
Monchepluton, Mt. Sopcha				
hole, 995/315	Olivinite, rock	17.00	6.25	0.16
hole, 995/315	Olivine	25.00	5.88	0.17
hole, 995/315	Orthopyroxene	31.00	6.25	0.16
hole, 995/315	Plagioclase	47.00	5.56	0.18
hole, 995/315	Magnetite	132.00	4.35	0.23
Monchepluton, dunite block				
hole, 904/102	Dunite, rock	218.00	1.47	0.68
hole, 904/102	Olivine	115.00	1.35	0.74
hole, 1651/244,9	Chromitite, ore	56.00	1.43	0.70
hole, C-1651/373,5*	Dunite-Bronzitite	28.00	0.83	1.20
hole, C-1622/7*	Chromitite, ore	2.80	0.69	1.44

Hole No/sampling depth (m)	Rock, mineral	$^4He10^{-6}$ µcm^3/g	$^4He/^3He10^6$	Low Mantle contribution**%
hole, C-1646/450*	Dunite	2.20	1.29	0.77
hole, C-1651/373.5*	Dunite-Bronzitite-contact	0.13	0.60	1.68

Note: errors are according to the calculation method (Tolstikhin and Marty, 1998).

*Step wise heating experiment (fraction under the temperature 1300C).

**Mantle components are given from value $^4He/^3He$ 0.55×10^4 (solar helium from lower mantle reservoir), Tolstikhin and Marty (1998).

Table 9 Isotopic $^4He/^3He$ ratios of PGE layered intrusions of the Baltic Shield.

12. Summary and conclusions

12.1. Total duration of magmatic activity, timing and multi-stages

The largest and richest ore deposits of the Monchepluton, Monchetundra and Fedorovo-Pansky Complexes have been carefully studied by geochronological methods.

The layered or differentiated series of mafic-ultramafic rocks, from troctolite to leucogabbro-anorthosite, and syngenetic Cu-Ni-PGE ores of the Monchepluton formed within the time interval of 2516 (max) to 2476 (min) Ma. Without analytical errors, the time interval is from 2507 Ma to 2493 Ma. Some researchers (Smolkin et al., 2004) suggest that the Vurechuaivench part of the pluton, composed of gabbroids and anorthosites containing PGE deposits, is an independent magma chamber and that the age of rock and syngenetic PGE ore emplacement is 2497±21 Ma.

The Fedorov Block of the Fedorovo-Pansky Complex represents an independent magma chamber, the rocks and ores of which differ significantly from those of the Western Pansky Block (Schissel et al., 2002; Nitkina, 2006; Serov et al., 2007).

The early magmatic activity about 2.5 Ga manifested itself in the gabbronorite of the Monchetundra (2505±6 Ma and 2501±8 Ma) and Mt. Generalskaya (2496±10 Ma). The magmatic activity that resulted in the formation of anorthosite took place about 2470 and 2450 Ma. It also contributed to the layered series of the Chunatundra (2467±7 Ma) and Mt. Generalskaya (2446±10 Ma), Monchetundra gabbro (2453±4 Ma; 2456±5 gabbro-anorthosite; and pegmatoid gabbronorite of the Ostrovsky intrusion (2445±11 Ma).

The Imandra lopolith is the youngest large layered intrusion within the Kola Belt. It varies from the other intrusions of the Kola Belt both in its emplacement age and its metallogeny. There are five U-Pb zircon and baddeleyite ages for the rocks of the main magmatic pulse represented by norite, gabbronorite, leucogabbro-anorthosite, gabbrodiorite, and granophyre; all formed within the interval from 2445 to 2434 Ma.

Thus, several eruptive pulses of magmatic activity have been established in the complex intrusions of the Kola Belt, including at least four pulses (or phases) in the Fedorovo-Pansky

Complex: a 2526-2516 Ma barren pulse, and three ore-bearing of 2505-2485 Ma, 2470 Ma, and 2450 Ma. For similar intrusions of the Fenno-Karelian Belt, for example, Penikat intrusion in Finland, five magmatic pulses varying only in geochemistry have been distinguished from the same deep chamber (Vogel et al., 1998; Iljina & Hanski, 2005).

A total duration for magmatic processes of over 80 million years in the Kola Belt intrusions is unexpected for many researchers.

The multi-phase magmatic duration of the Fenno-Karelian Belt intrusions was short-term and took place about 2.44 Ga years ago. However, there are only a few U-Pb precise age estimations for the Fenno-Karelian Belt intrusions (Iljina & Hanski, 2005). A joint Russian-Finnish research collaboration intended for dating the intrusions of the both belts has recently been initiated. It is expected that the research will result in updating the knowledge about the timing and duration of the Paleoproterozoic ore-forming intrusions on the Baltic Shield.

The Kola results underline that the layering of the intrusions with thinly-differentiated horizons and PGE reefs was not contemporaneous (or syngenetic) with each intrusion defining its own metallogentic trends in time and space.

12.2. Metallogeny features

The Palaeoproterozoic magmatic activity in the eastern Baltic Shield is associated with the formation of widespread ore deposits: Cu-Ni (±PGE), Pt-Pd (±Rh, ±Cu, Ni, Au), Cr, Ti-V (Richardson & Shirey, 2008; Mitrofanov & Golubev, 2008).

On the Kola Peninsula, economic Cu-Ni (±PGE) deposits are known in the Monchegorsk (~2500 Ma) and Pechenga (~1980 Ma) type intrusions. In the Monchepluton (the Monchegorsk type), syngenetic disseminated Cu-Ni (±PGE) ore bodies of magmatic origin are confined to basal parts of magmatic chambers (Papunen & Gorbunov, 1985), while massive rich redeposited ores in the veined bodies of the Monchepluton bottom as well as beyond it (offset bodies) also contain a relatively high portion of platinum among platinum-group elements. They are associated mainly with ca. 2500 Ma magnesia-rich mafic-ultramafic rocks with ε_{Nd} (2.5 Ga) values varying from-1 to-2. In comparison, Cu-Ni (±PGE) ores of the Pechenga type intrusions that are not discussed are related to the 1980 Ma gabbro-wehrlite rocks with ε_{Nd}(1.98 Ga) values varying from ±1 to ±3 (Hanski et al., 1990; Mitrofanov & Golubev, 2008). The basal ores of the Fedorovo deposit are first of all valuable for platinum-group elements (Pt, Pd, Rh), but nickel, copper and gold are also of economic importance here (Schissel et al., 2002).

Pt-Pd (±Cu, Ni, Rh, Au) reef-type deposits and ore occurrences of the Vurechuaivench Foothills (Monchepluton) and Western Pansky Block (Fedorovo-Pansky Complex) seem, in terms of genesis, to be associated with pegmatoid leucogabbro and anorthosite rocks enriched in late-stage fluids. Portions of this magma produce additional injections of ca. 2500 Ma (Vurechuaivench), ca. 2470 Ma (the Lower, Northern PGE reef), and ca. 2450 Ma (the Upper, Southern PGE reef of the Western Pansky Block and PGE-bearing mineralization of the Mt. Generalskaya intrusion). These nonsimultaneous injections are quite close in terms of composition, prevalence of Pd over Pt, ore mineral composition (Mitrofanov et al., 2005), and isotope geochemistry

of Sm-Nd and Rb-Sr systems. The ε_{Nd} values for the rocks under consideration vary from-1 to-3, which probably indicates a single long-lived magmatic hearth.

Chromium concentration (>1000 ppm) is typical geochemical feature of the lower mafic-ultramafic rocks of the layered intrusions of the Baltic Shield (Alapieti, 1982; Iljina & Hanski, 2005). The chromite mineralization is known in the basal series of the Monchepluton, Fedorovo-Pansky Complex, Imandra lopolith (Russia), Penikat and Narkaus intrusions (Finland) and in chromite deposits of the Kemi intrusion (Finland) and Dunite Block (Monchepluton, Russia). On the contrary, Fe-Ti-V mineralization of the Mustavaara intrusion (Finland) tends to most leucocratic parts of the layered series, and to leucogabbro-anorthosite and gabbro-diorite of the Imandra lopolith (Russia) and Koillismaa Complex (Finland).

Thus, PGE-bearing deposits of the region are represented by two types: the basal and the reef-like ones. According to modern economic estimations, the basal type of deposits is nowadays more preferable for mining, even if the PGE concentration (1-3 ppm) is lower compared to the reef-type deposits (>5ppm). Basal deposits are thicker and contain more platinum, copper and, especially, nickel. These deposits are accessible to open pit mining.

12.3. Isotope-geochemistry and geodynamic significance

Magmatic processes since the Palaeoproterozoic (2.53 Ga) have affected almost the whole region of the East-Scandinavian (Kola-Lapland-Karelian) province and a mature continental crust formed (2.55 Ga) in the Neoarchaean (Gorbatschev & Bogdanova, 1993). Thick (up to 3 km) basaltic volcanites of the Sumian age (2.53-2.40 Ga) in Karelia, Kola and northeast Finland cover an area of greater than 200.000 km^2. In the north, magmatic analogues of these volcanic rocks are represented by two belts of layered intrusions and numerous dyke swarms (Vuollo et al., 2002, Vuollo & Huhma, 2005). This together composes a single time-and space-related megacyclic association, the East-Scandinavian Large Igneous Province (LIP). All the magmatic units of the province covering a huge area show similar geological, compositional and metallogenic features (Coffin, Eldholm, 1994).

Regional geological settings indicate anorogenic rift-like intraplate arrangements involving volcano-plutonic belts connecting different domains of the Paleoarchaean Kola-Lapland-Karelia protocontinent. This resembles early advection extensional geodynamics of passive rifting that is typical of intraplate plume processes (Pirajno, 2007).

Geochemical and isotope-geochemical data shed light on features of deep magma source for the LIP rocks. T_{DM} values (Faure, 1986) are approximately the age of the depleted mantle reservoir (DM) with slightly enriched Sm-Nd ratios. The T_{DM} values lie within the interval of 3.1-2.8 Ga. The ε_{Nd} values vary from-1.1 to-2.4 and similar I_{Sr} values (0.703-0.704) obtained for discrete layered intrusions form a narrow range of enriched compositions. It is difficult to argue for a local crustal contamination and we suggest that the magmas producing different rocks of the LIP layered intrusions were derived from a single homogenous mantle source enriched both with typically magmatic ore elements (Ni, TI, V, and Pt) and lithophile elements including light REE. To some extent, this reservoir is comparable with the modern EM-1 source (Hofmann, 1997).

Isotope $^4He/^3He$ ratio is also a reliable isotope tracer of mantle plume processes (Tolstikhin & Marty, 1998; Bayanova et al., 2006, 2009; Pirajno, 2007). Their use in studying Precambrian rocks and requires special case. Table 9 shows recent helium isotope data for the rocks and minerals of the Kola Belt intrusions. The data indicate that the $^4He/^3He$ isotope ratios of n x 10^{6-5} correspond to those of the upper mantle and differ from those of the crust (n x 10^8) and lower mantle (n x 10^4) (Tolstikhin & Marty, 1998). The helium isotope data tend to favour a source dominated by mantle derived magmas with only local crustal contamination.

According to the available data (Campbell, 2001; Condie, 2001; Vuollo et al., 2002; Bleeker, 2003; Ernst & Buchan, 2003; Bleeker, Ernst, 2006; Bayanova et al., 2009; present study), the peak of the mafic-ultramafic magmatic activity of the Kola-Karelian, Superior and Wyoming provinces has been estimated at ~2.45 Ga. Figure 12 presents an attempt to demonstrate some reconstruction of the Archaean supercontinent embodying these three provinces of Europe and North America (Heaman, 1997; Bleeker, Ernst, 2006; Ernst, 2008). Trends of the Kola and Fenno-Karelian Belts of 2.52-2.44 Ga layered intrusions are show with the intraplate nature interpreted from the results of the present study.

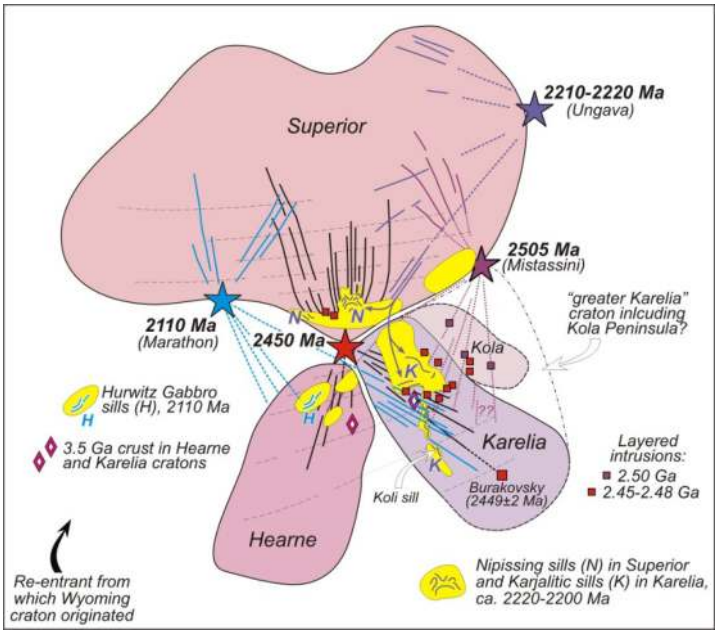

Figure 12. A new correlation for the Superior, Karelia and Hearne craton. The detailed fit is based on successful matching of several short-lived magmatic events, at ca. 2450 Ma (Matachewan), ca. 2217 Ma (Nipissing (N) and Karjalitic (K) sills), and ca. 2110 Ma (Marathon), as well as correlation of the cover sequences (see text). Kola is likely part of this correlation as part of a "greater Karelia" craton. The Wyoming craton likely originated from the re-entrant west of the Hearne craton. Note that our reconstruction successfully places the ca. 3.5 Ga Siurua gneiss of Karelia (diamond symbol; "Europe's oldest rocks") along strike of similar age crust in the Hearne craton. Arrows indicate part of the long-distance transport of magma to feed the Nipissing and Karjalitic sills (Bleeker, Ernst, 2006).

The LIP layered intrusions are directly related to the Baltic Shield metallogeny (Mitrofanov & Golubev, 2008). The >80 Ma duration and multiphase history of the Kola Belt layered mafic intrusions (i.e., 2.53-to 2.45 Ga) has been shown here. It has also been underlined that the younger intrusions of the Fenno-Karelian Belt (Fig. 1) cluster at 2.44 Ga (Iljina & Hanski, 2005). The partially asynchronous evolution of these two belts, that are thought to be arms of a mantle plume, is now being examined in more detail as a follow-up to this study within the framework of Russian-Finnish and Canadian research collaboration (Ernst, 2008).

A number of new U-Pb and Sm-Nd isotope data were obtained for Monchetundra massif of Monchegorsk ore region and various rocks of the mafic layered intrusions of the Kola Belt (Baltic Shield), including those which bear PGE, Ni-Cu and Ti-V mineralization. A surprisingly long period of multiphase magmatic activity, from 2530 to 2450 Ma (about 80 million years), resulted in the intrusion of large-scale ore-bearing intrusions of the Kola Belt. Magmatism continued until about 2400 Ma and generated wide-spread dykes and small-scale intrusions. These results contrast with the published data indicating short-term evolution interval (~2440 Ma) for similar intrusions of the Fenno-Karelian Belt (Iljina & Hanski, 2005).

The two belts of mafic layered intrusions of the Baltic Shield (the Kola and Fenno-Karelian belts), together with the surrounding volcanic rocks and dyke swarms, compose the Palaeoproterozoic East-Scandinavian Large Igneous Province (LIP) with an area of more than 200.000 km^2. The petrological-geodynamic interpretation proposed by the present paper of the LIP is a product of a vast long-lived plume is based on the enriched isotope characteristics of the magmas and also the large volume and widespread distribution of the magmas. The is acknowledge that alternatives involving super-long duration of the homogenous deep-seated magma sources are possible.

13. Discussion

13.1. Specific features of the isotope investigation of the intrusions

The U–Pb concordia and isochron method has been used to define the age of crystallization of the rocks. The values obtained on zircons and baddeleyites from the same sample usually lie at the isochron, indicating a similar age of magma crystallization and subsequent transformations. Coordinates of baddeleyites are near the Concordia line. However, the method encounters the obstacle that mafic rocks contain very few zircon and baddeleyite grains. Samples of tens of kilograms yield only a few milligrams of these minerals.

In order to compare our U–Pb results (23 isochron points), some samples were sent to the

Royal Ontario Museum Laboratory in Canada. The data obtained there (Amelin et al. 1995) agree with ours within error.

The Sm–Nd system is not an accurate geochronometer (c. 2–5%). However, the Sm–Nd isochron method can allow the establishment of crystallization times for mafic rocks on major rock-forming minerals (olivine, orthopyroxene, clinopyroxene and plagioclase). It is especially

important for dating rocks with syngenetic ore minerals. For example, this method has been used to determine for the first time the age (2482±36 Ma) of the early ore body in the Fedorovo-Pansky Cu–Ni–PGE deposit of the Kola Peninsula that has economic importance (Serov et al. 2007).

For the mafic-ultramafic intrusions of the Kola belt, the Sm–Nd ages overlap because of high errors, but are coμmonly close to the U–Pb (TIMS) data on zircon and baddeleyite. They are especially valid for the marginal fast-crystallizing rocks of the Taxitic Zone of the Fedorovo-Pansky Complex, where the early barren orthopyroxenite and gabbro have the following ages: 2521±42 Ma and 2516±35 Ma (Sm–Nd method) and 2526±6 Ma and 2516±7 Ma (U–Pb method), respectively. The ore-bearing norite of the Fedorov Block yielded an age of 2482±36 Ma (Sm–Nd method) and 2485±9 Ma (U–Pb method) according to Nitkina (2006) and Serov et al. (2007).

It is also important to stress that the Sm–Nd method provides valuable petrological and geochemical markers: $\varepsilon_{Nd}(T)$ and T_{DM}. The ε_{Nd} shows the degree of mantle magma source depletion, while T_{DM} indicates an approximate age of the mantle protolith (Faure 1986).

The Rb–Sr whole rock and mineral isochron method is mostly valuable for dating unaltered felsic igneous rocks and metamorphic amphibolitefacies associations (Faure 1986). In our work, 9 Rb–Sr isotope values for the rocks are considered to have only a petrological implication. Together with specific trace elements (Cu, Ni, Ti, V and LREE), ε_{Nd} (2.5 Ga) and $^{4}He/^{3}He$ data, the values of initial $^{87}Sr/^{86}Sr$ (I_{Sr} [2.5 Ga]) indicate an enriched mantle reservoir 2.5 billion years ago which is comparable with the modern EM-I.

13.2. The timing, pulsation and total duration of magmatic activity

The largest and richest ore deposits of the Monchepluton and Fedorovo-Pansky complexes have been carefully studied by geochronological methods.

The layered or differentiated series of maficultramafic rocks, from troctolite to leucogabbroanorthosite, and syngenetic Cu–Ni–PGE ores of the Monchepluton formed within the time interval of 2516 (max)–2476 (min) Ma. Without analytical errors, the time interval is from 2507–2493 Ma. Some researchers (Smolkin et al. 2004) suggest that the Vurechuaivench part of the pluton, composed of gabbroids and anorthosites containing PGE deposits, is an independent magma chamber and that the age of rock and syngenetic PGE ore emplacement is 2497±21 Ma.

The Fedorov Block of the Fedorovo-Pansky Complex represents an independent magma

chamber, the rocks and ores of which differ significantly from those of the Western Pansky Block (Schissel et al. 2002). The 2 km-thick rock sequence, from the Marginal Zone to the Lower Gabbro Zone, is a layered or differentiated syngenetic series of relatively melanocratic pyroxenite-norite-gabbronorite-gabbro dated at 2526±6 and 2516±7 Ma. The Taxitic Zone is penetrated by concordant and cutting Cu–Ni–PGEbearing gabbronorite (Fedorovo deposit) of the second pulse of magmatic injection, which is slightly younger (2485±9 Ma.

The Western Pansky Block from the Main Gabbronorite Zone, without the Lower Layered Horizon and probably without the upper part (above 3000 m), can also be considered a single syngenetic series of relatively leucocratic, mainly olivine-free gabbronorite-gabbro crystallized

within the interval of 2503–2498–2491±5 Ma. In the lower part of the Block there are Norite and Marginal zones. The Marginal zone contains poor disseminated Cu–Ni–PGE mineralization. This rock series can be correlated with certain parts of the Monchepluton and the Fedorov Block. The 40–80 m-thick Lower Layered Horizon (LLH) is prominent because of its contrasting structure with predominant leucocratic anorthositic rocks. The exposed part of the horizon strikes for almost 15 km and can be traced in boreholes down to a depth of 500 m (Mitrofanov et al. 2005). By its morphology, the horizon seems to be part of a single layered series. Nevertheless, there are anorthositic bodies that in outcrop show cutting contacts and apophyses (Latypov & Chistyakova 2000); the cumulus plagioclase compositions in the rocks of the horizon are different from those in the surrounding rocks; and the age of the PGE-bearing leucogabbro-pegmatite, which is precisely defined by concordant and near-concordant U–Pb data on zircon as 2470±9 Ma, is slightly younger than the ages of the surrounding rocks (e.g. 2491±1.5 Ma). The LLH rocks, especially the anorthosite and the PGE mineralization, probably represent an independent magmatic pulse.

The upper part and olivine-bearing rocks of the Western Pansky Block and the anorthosite of the Upper Layered Horizon (ULH) with the Southern PGE Reef have been poorly explored. They differ from the main layered units of the Block in rock, mineral and PGE mineralization composition (Mitrofanov et al. 2005). Until now, only one reliable U–Pb age (2447±12 Ma) has been obtained for the PGE-bearing anorthosite of the block, which may represent another PGEbearing magmatic pulse.

The early magmatic activity of about 2.5 Ga manifested itself in the gabbronorite of the Monchetundra (2505±6 and 2501±8 Ma) and Mt Generalskaya (2496±10 Ma). The magmatic activity that resulted in the formation of anorthosite took place about 2470 and 2450 Ma. It also contributed to the layered series of the Chunatundra (2467±7 Ma) and Mt Generalskaya (2446±10 Ma), Monchetundra gabbro (2453±4 Ma, Mitrofanov et al. 1993) and pegmatoid gabbronorite of the Ostrovsky intrusion 2445±11 Ma.

The Imandra lopolith is the youngest large layered intrusion within the Kola Belt. It varies from the other intrusions of the Kola Belt both in its emplacement age and its metallogeny. There are five U–Pb zircon and baddeleyite ages for the rocks of the main magmatic pulse represented by norite, gabbronorite, leucogabbro-anorthosite, gabbrodiorite and granophyre; all formed within the interval from 2445–2434 Ma.

Thus, several eruptive pulses of magmatic activity have been established in the complex intrusions of the Kola Belt, including at least four pulses (or phases) in the Fedorovo-Pansky Complex: a 2526–2516 Ma barren pulse and three ore-bearing of 2505–2485, 2470 and 2450 Ma. For similar intrusions of the Fenno-Karelian Belt, for example, the Penikat intrusion in Finland, five magmatic pulses varying only in geochemistry have been distinguished from the same deep chamber (Iljina & Hanski 2005).

A total duration for magmatic processes of over 130 Ma in the Kola Belt intrusions is unexpected for many researchers. The multi-phase magmatic duration of the Fenno-Karelian Belt intrusions was short-term and took place about 2.44 Ga years ago. However, there are only a few U–Pb precise age estimations for the Fenno-Karelian Belt intrusions (Iljina & Hanski

2005). A joint Russian– Finnish research collaboration intended for dating the intrusions of the both belts has recently been initiated. It is expected that the research will result in updating the knowledge about the timing and duration of the Palaeoproterozoic ore-forming intrusions on the Baltic Shield.

The Kola results underline that the layering of the intrusions with thinly-differentiated horizons and PGE reefs was not contemporaneous (or syngenetic), with each intrusion defining its own metallogentic trends in time and space.

13.3. Metallogenic implications

The Palaeoproterozoic magmatic activity in the eastern Baltic Shield is associated with the formation of widespread ore deposits: Cu–Ni (±PGE), Pt–Pd (.Rh, ±Cu, Ni, Au), Cr, Ti–V (Mitrofanov & Golubev 2008; Richardson & Shirey 2008).

On the Kola Peninsula, economic Cu–Ni (+PGE) deposits are known in the Monchegorsk (c. 2500 Ma) and Pechenga (c. 1980 Ma) type intrusions. In the Monchepluton (the Monchegorsk type), syngenetic disseminated Cu–Ni (+PGE) ore bodies of magmatic origin are confined to basal parts of magmatic chambers (Papunen & Gorbunov 1985), while massive rich redeposited ores in the veined bodies of the Monchepluton bottom as well as beyond it (offset bodies) also contain a relatively high portion of platinum among PGE. They are associated mainly with c. 2500 Ma magnesium-rich mafic-ultramafic rocks with 1Nd (2.5 Ga) values varying from 21 to 22. In comparison, Cu–Ni (±PGE) ores of the Pechenga type intrusions, that are not discussed, are related to the 1980 Ma gabbro-wehrlite rocks with 1Nd (1.98 Ga) values varying from+1 to+3 (Hanski et al. 1990; Mitrofanov & Golubev 2008). The basal ores of the Fedorovo deposit are first of all valuable for platinum-group elements (Pt, Pd, Rh), but nickel, copper and gold are also of economic importance here (Schissel et al. 2002). The ore-forming magmatic and post-magmatic processes are closely related to the Taxitic Zone gabbronorite of 2485±9 Ma magmatic pulse.

Pt–Pd (±Cu, Ni, Rh, Au) reef-type deposits and ore occurrences of the Vurechuaivench Foothills (Monchepluton) and Western Pansky Block (Fedorovo-Pansky Complex) seem, in terms of genesis, to be associated with pegmatoid leucogabbro and anorthosite rocks enriched in late-stage fluids. Portions of this magma produce additional injections of c. 2500 Ma (Vurechuaivench), c. 2470 Ma (the Lower, Northern PGE reef) and c. 2450 Ma (the Upper, Southern PGE reef of the Western Pansky Block and PGE-bearing mineralization of the Mt Generalskaya intrusion). These nonsimultaneous injections are quite close in terms of composition, prevalence of Pd over Pt, ore mineral composition (Mitrofanov et al. 2005), and isotope geochemistry of Sm–Nd and Rb–Sr systems. The ε_{Nd} values for the rocks under consideration vary from 21 to 23, which probably indicates a single long-lived magmatic hearth.

Chromium concentration (.1000 ppm) is a typical geochemical feature of the lower maficultramafic rocks of the layered intrusions of the Baltic Shield (Alapieti 1982; Iljina & Hanski 2005). The chromite mineralization is known in the basal series of the Monchepluton, Fedorovo-Pansky Complex, Imandra lopolith (Russia), Penikat and Narkaus intrusions (Finland) and in chromite deposits of the Kemi intrusion (Finland) and Dunite Block (Monchepluton,

Russia). On the contrary, Fe–Ti–V mineralization of the Mustavaara intrusion (Finland) tends to most leucocratic parts of the layered series, and to leucogabbro-anorthosite and gabbro-diorite of the Imandra lopolith (Russia) and Koillismaa Complex (Finland).

Thus, PGE-bearing deposits of the region are represented by two types: the basal and the reef-like ones. According to modern economic estimations, the basal type of deposits is nowadays more preferable for mining, even if the PGE concentration (1–3 ppm) is lower compared to the reef-type deposits (>5 ppm). Basal deposits are thicker and contain more platinum, copper and, especially, nickel. These deposits are accessible to open pit mining.

13.4. Petrological and geodynamic implications

Magmatic processes since the Palaeoproterozoic (2.53 Ga) have affected almost the whole region of the East Scandinavian (Kola-Lapland-Karelian) province and a mature continental crust formed (2.55 Ga) in the Neoarchaean (Gorbatschev & Bogdanova 1993). Thick (up to 3 km) basaltic volcanites of the Sumian age (2.53–2.40 Ga) in Karelia, Kola and NE Finland cover an area of >200 000 km^2. In the north, magmatic analogues of these volcanic rocks are represented by two belts of layered intrusions and numerous dyke swarms (Vuollo et al. 2002; Vuollo & Huhma 2005). This together composes a single time-and space-related megacyclic association, the East Scandinavian Large Igneous Province (LIP). All the magmatic units of the province covering a huge area show similar geological, compositional and metallogenic features.

Regional geological settings indicate anorogenic rift-like intraplate arrangements involving volcanoplutonic belts connecting different domains of the Palaeoarchaean Kola-Lapland-Karelia protocontinent. This resembles early advection extensional geodynamics of passive rifting that is typical of intraplate plume processes (Pirajno 2007). Geochemical and isotope-geochemical data shed light on features of deep magma source for the LIP rocks. TDM values (Faure 1986) are approximately the age of the depleted mantle reservoir (DM) with slightly enriched Sm–Nd ratios. The TDM values lie within the interval of 3.1–2.8 Ga. The ε_{Nd} values vary from-2.4 to+1.2 and similar I_{Sr} values (0.703–0.704) obtained for discrete layered intrusions form a narrow range of enriched compositions. It is difficult to argue for a local crustal contamination and we suggest that the magmas producing different rocks of the LIP layered intrusions were derived from a single homogenous mantle source enriched both with typically magmatic ore elements (Ni, TI, V and Pt) and lithophile elements including light REE. To some extent, this reservoir is comparable with the modern EM-1 source (Hofmann 1997).

Isotope^{4}He/^{3}He ratio is also a reliable isotope tracer of mantle plume processes (Tolstikhin & Marty 1998; Bayanova et al. 2006; Pirajno 2007). Their use in studying Precambrian rocks requires special care. Table 10 shows recent helium isotope data for the rocks and minerals of the Kola Belt intrusions. The data indicate that the ^{4}He/^{3}He isotope ratios of n × 10$^{6–5}$ correspond to those of the upper mantle and differ from those of the crust (n × 10^8) and lower mantle (n × 10^4) (Tolstikhin & Marty 1998). The helium isotope data tend to favour a source dominated by mantle-derived magmas with only local crustal contamination.

According to the available data (Campbell 2001; Condie 2001; Vuollo et al. 2002; Bleeker 2003; Ernst & Buchan 2003; present study), the peak of the mafic-ultramafic magmatic activity of the Kola-Karelian, Superior and Wyoming provinces has been estimated at c. 2.45 Ga. Fig. 12 presents an attempt to demonstrate some reconstruction of the Archaean supercontinent embodying these three provinces of Europe and North America (Heaman 1997; Bleeker, Ernst, 2006). Insert (A) shows trends of the Kola and Fenno-Karelian Belts of 2.52–2.40 Ga layered intrusions with the intraplate nature interpreted from the results of the present study.

The LIP layered intrusions are directly related to the Baltic Shield metallogeny (Mitrofanov & Golubev 2008). The 130 Ma duration and multiphase history of the Kola Belt layered mafic intrusions (i.e. 2.53–2.40 Ga) has been shown here. It has also been underlined that the younger intrusions of the Fenno-Karelian Belt clustre at 2.44 Ga (Iljina & Hanski 2005). The partially asynchronous evolution of these two belts, that are thought to be arms of a mantle plume, is now being examined in more detail as a follow-up to this study within the framework of Russian-Finnish research collaboration.

5. Relationship of Pt-Pd provinces with large igneous provinces, LIP (hot plume fields)

Large igneous provinces (or LIPs, by Campbell, Griffiths, 1990) as derivatives of deep mantle plume or asthenospheric upwelling processes were minutely discussed in May 2006 in China at the International Continental Volcanism Conference (Yi-gang Xu, 2007). A special LIP group along with alkaline, komatiite, felsic ones, is represented by mafic intraplate continental provinces (or mafic LIPs, by Bleeker, Ernst, 2006) composed of thick riftogene sedimentary and volcanic rocks cogenetic with dike swarms and mafic-ultramamfic intrusions.

Grachyov (2003), Pirajno (2007), Bogatikov et al. (2010) cite main geological, geophysical, and geochemical features of geological processes within LIPs related with deep mantle plumes. Taking into account experience of studying ancient (Precambian) areas where most geological and geophysical features of geological units, bodies, and rock compositions fail to be preserved, Felix P. Mitrofanov proposed the following indicators of various rank for intraplate mafic LIPs:

- presence of gravitational anomalies caused by a crust-mantle layer in the crust bottom;
- riftogene (anorogenic) structural ensemble with manifestations of multipath fault tension tectonics identified by the distribution of grabens and volcanic belts, elongated dike swarms, and radial belts of intrusions;
- long duration, polystage and pulsating nature of tectonics and magmatism, continental discontinuities and erosion with early stages of tholeiite-basalt (trappean), boninite-like and subalkaline magmatism in the continental crust, and possible closing stages of the Red Sea spreading magmatism;
- intrusive sills, lopoliths, sheet-like bodies, large dikes and dike swarms. The intrusions are often layered, being different from rocks typical of subduction and spreading zones in terms of nature (Bleeker, Ernst, 2006), with trends of thin differentiation (or layering), with limited development of intermediate and felsic rocks, often with leucogabbro and anorthosite ends and abundant pegmatoid mafic varieties;

- typical mantle geochemistry of rocks and ores, isotope mantle tracers: $^{143}Nd/^{144}Nd$, $^{87}Sr/^{86}Sr$, $^{187}Os/^{188}Os$, $^{3}He/^{4}He$;
- mafic intracontinental LIPs accoμmodate large orthomagmatic Cr, Ni, Cu, Co, PGE (±Au), Ti, V deposits.

The Palaeoproterozoic East-Scandinavian Large Igneous Province (LIP) with a modern area of ca. 1,000,000 km^2 occupies the eastern part of the Baltic (or Fennoscandinavian) Shield which basement is represented by the mature Archaean granulite and gneiss-migmatite crust formed > 2550 Ma. Main features of the structure and description of coμmercial Pt-Pd and Cu-Ni-PGE deposits are given in modern publications of F. Mitrofanov, Ye. Sharkov, V. Smolkin, A. Korchagin, T. Bayanova, S. Turchenko, etc. It is worth noting certain preserved geological and geophysical features of this ancient (Palaeoproterozoic) ore-bearing mafic LIP.

Geophysical survey demonstrated the lower part of the Earth crust in the eastern part of the shield to be represented by a transitional crust-mantle layer (Vp=7.7-7.1 km/s). Deep xenoliths in the Kandalaksha explosion pipes elevated from this layer have the compositions of granulite and garnet anorthosite with an age of 2460 Ma typical of most bodies in the province (Verba et al., 2005). This shows that masses of deep matter arose not only in the form of volcanic, dikes, and intrusions, but also emplaced to the crust bottom in the course of vast underplating (Mitrofanov, 2010). The outcropped part of the province continues under the platform cover in the northern part of the Russian platform in the form of vast Palaeoproterozoic Baltic-Central Russian wide arc, or intracontinental orogen (Mints, 2011). This certainly expands long-term coμmercial opportunities of the province.

Anorogenic autonomous pattern of grabens, dike swarms and belts (rays) of intrusive bodies independent from the structure of the enclosing Archaean gneiss-migmatite frame, is prominent in the Geological Map of the Fennoscandian Shield (2005). The studied intrusions with deposits and prospects compose elongated belts (rays), e.g. northwesttrending Kola belt in the northern part of the province, and northeasttrending Fenno-Karelian belt with the concentration of intrusions in the well-known Monchegorsk ore node (Bayanova et al., 2009).

In the Early Palaeoproterozoic (2530-2400 Ma) epoch of the long history of the LIP evolution, a few stages separated by breaks (conglomerates) sedimentation and magmatism have been distinguished. The Sumi (2550-2400 Ma) stage was principle in the metallogeny of Pt-Pd ores related to the intrusive siliceous highly Mg boninite-like and anorthositic magmatism (Mitrofanov, 2005; Sharkov, 2006). Such ore-bearing intrusions formed earlier in the Kola belt (Fedorov-Pana and other intrusions: 2530-2450 Ma) and later in the Fenno-Karelian belt (2450-2400 Ma), according to (Bayanova et al., 2009; Mitrofanov et al., 2012; Ekimova et al., 2011).

A number of new U–Pb and Sm–Nd isotope data were obtained for various rocks of the mafic layered intrusions of the Kola Belt (Baltic Shield), including those which bear PGE, Ni–Cu and Ti–V mineralization. A surprisingly long period of multiphase magmatic activity, from 2530–2400 Ma (about 130 Ma), resulted in the intrusion of large-scale ore-bearing

intrusions of the Kola Belt. Magmatism continued until about 2400 Ma and generated widespread dykes and small-scale intrusions. These results contrast with the published data, indicating short-term evolution interval (c. 2440 Ma) for similar intrusions of the Fenno-Karelian Belt (Iljina & Hanski 2005).

The two belts of mafic layered intrusions of the Baltic Shield (the Kola and Fenno-Karelian belts), together with the surrounding volcanic rocks and dyke swarms, compose the Palaeoproterozoic East Scandinavian Large Igneous Province (LIP) with an area of >200 000 km^2. The petrologicalgeodynamic interpretation proposed by this chapter of the LIP is a product of a vast longlived plume is based on the homogenous and enriched isotope characteristics of the magmas and also the large volume and widespread distribution of the magmas. It is quite possible, and fully consistent with our observations, that the geochemical signatures of the LIP magmas may well have been in part inherited from the subcontinental lithosphere, as described recently based on Osisotope characteristics for the Bushveld magmas (Richardson & Shirey 2008).

Acknowledgements

We thank to D.Wasserburg for ^{205}Pb artificial spike, J. Ludden for 91500 and Temora standards, F. Corfu, V. Todt and U. Poller for assistance in the establishing of the U-Pb method for single zircon and baddeleyite grains.

The authors would like to thank the following: L. Koval for baddeleyite, zircon, rock-forming and sulphides minerals separation from rock samples; L. Laylina for baddeleyite and zircon analyses using a Cameca MS-46 and for taking images of baddeleyite crystals; N. Levkovich for the chromatographic separation of U and Pb for analyses by mass spectrometry at the Geological Institute, Kola Science Center, Russian Academy of Sciences.

The studies were supported by the Russian Foundation of Basic researches (RFBR), projects no. 13-05-00493, OFI-M-13-05-12055, IGCP-SIDA-599 and Program Department of Earth Sciences RAS no. 2, 4.

Author details

T. Bayanova, F. Mitrofanov, P. Serov, L. Nerovich, N. Yekimova, E. Nitkina and I. Kamensky

*Address all correspondence to: tamara@geoksc.apatity.ru

Geological Institute of the Kola Science Centre, Russian Academy of Sciences (GI KSC RAS), Apatity, Russia

References

[1] Alapieti, T.T. 1982. The Koillismaa layered igneous complex, Finland: its structure, mineralogy and geochemistry, with emphasis on the distribution of chromium. Geol. Surv. Finland, Bull. 319, 116.

[2] Alapieti, T.T., Filen, B.A., Lahtinen, J.J., Lavrov, M.M., Smolkin, V.F. & Voitekhovsky, S.N. 1990. Early Proterozoic layered intrusions in the Northeastern part of the Fennoscandian Shield. Miner. Petrol., 42, 1-22.

[3] Amelin, Yu.V., Heaman, L.M & Semenov, V.S. 1995. U-Pb geochronology of layered mafic intrusions in the eastern Baltic Shield: implications for the timing and duration of Palaeoproterozoic continental rifting. Precambrian Research, 75, 31-46.

[4] Balashov, Y.A., Bayanova, T.B., & Mitrofanov, F.P. 1993. Isotope data on the age and genesis of layered basic-ultrabasic intrusions in the Kola Peninsula and northern Karelia, northeastern Baltic Shield. Precambrian Research, 64, N ¼, 197-205.

[5] Bayanova, T.B. 2004. Age of reference Geological complexes of the Kola region and the duration of igneous processes. Saint-Petersburg, Nauka, 174.

[6] Bayanova, T.B., Nerovich, L.I., Mitrofanov, F.P., Zhavkov, V.A., Serov, P.A. The Monchetundra basic massif of the Kola region: new geological and isotope geochronological data // Doklady Earth Sciences, 2010. V. 431. N 1. C. 288-293.

[7] Bayanova, T., Ludden, J. & Mitrofanov, F. 2009. Timing and duration of Palaeoproterozoic events producing ore-bearing layered intrusions of the Baltic Shield: metallogenic, petrological and geodynamic implications / In: Reddy S.M., Mazumder R., Evans D.A.D. & Collins A.S. (eds) // Palaeoproterozoic Supercontinents and Global Evolution. Geological Society, London, Special Publications, 323, 165-198.

[8] Bayanova, T.B, Novikov D.D., Nitkina, E.A., Serov, P.A. & Mitrofanov, F.P. 2006. Polychronic and long-time interval of the Formation Proterozoic PGE – bearing Fedorovo-Pansky intrusion. Understanding the genesis of ore deposits to meet the demands of the 21st century. 12th quadrennial IAGOD symposium 2006: Abstract. Moscow. (fill №106).

[9] Bayanova, T.B. & Mitrofanov, F.P. 2005. Layered Proterozoic PGE intrusions in Kola region: new isotope data. X international symposium of platinum "Platinum-Group Elements - from Genesis to Beneficiation and Environmental Impact": Extended abstracts. Oulu, Finland, 289-291.

[10] Bayanova, T.B. 2006. Baddeleyite: A Promising Geochronometer for Alkaline and Basic Magmatism. Petrology. 14, N 2, 187-200.

[11] Bayanova, T.B., & Balashov, Yu.A 1995. Geochronology of Palaeoproterozoic layered intrusions and volcanites of the Baltic Shield: Proceed. of the 1 st. Intern. Barents

Sympos. "Geology and minerals in the Barents Region". Norges geol. unders. Spec. Publ. 7, 75-80.

[12] Bayanova, T.B., Galimzyanova, R.M. & Fedotov, G.A. 2001. Evidence of the multiphase complex history of the Imandra lopolith. Svekalapko. Europrobe project. 6th Workshop. Abstracts. Laμmi, Finland. University of Oulu, 7.

[13] Bayanova, T.B., Smolkin, V.F. & Levkovich, N.V. 1999. U-Pb geochronological study of Mount Generalskaya layered intrusion, northwestern Kola Peninsula, Russia. Transactions of the Institution of Mining and Metallurgy, 108, B83-B90.

[14] Bleeker, W., Ernst, R. 2006. Short-lived mantle generated magmatic events and their dyke swarms: the key unlocking Earth's paleogeographic record back to 2.6 Ga. Dyke Swarms-Time Marker of Crustal Evolution, Balkema Publ. P.1-20.

[15] Bleeker, W. 2003. The late Archaean record: a puzzle in ca. 35 pieces. Lithos. 71, 99-134.

[16] Bogatikov, O.A., Kovalenko, V.I., Sharkov, Ye.V. 2010. Magmatism, tectonics, and geodynamics of the Earth. M., Nauka, 606 p.

[17] Boynton, W.V. 1984. Cosmochemistry of the rare earth elements: meteorite studies / Ed. Henderson P. Rare earth element geochemistry. Amsterdam: Elsevier, 63-114.

[18] Campbell, L.H., Griffiths, R.W. 1990. Implications of mantle plume structure for the evolution of flood basalts. Earth and Planetary Science Letters. V. 99. P. 79-93.

[19] Campbell, I.H. 2001. Identification of ancient mantle plumes. In Ernst R.E. and Buchan (Eds.) Mantle plumes: their identification through time. Geological Society of America, Special Papers. 352, 5-22.

[20] Chashchin, V.V., Bayanova, T.B. & Apanasevich, E.A. 2002. The Monchegorsk Ore District as an Example of the Palaeoproterozoic Ore-bearing Chamber Structure (Kola, Russia). Geology of Ore Deposits, 44, N 2, 142-149.

[21] Coffin, M.F. & Eldholm, O. 1994. Large igneous provinces: crustal structure, dimensions and external consequences. Rev. Geophys., 32, 1-36.

[22] Condie K.C. Supercontinents and superplume events: Distinguishing signals in the geology record. Phys. of the Earth and Planetary Interiors, v.146, p.319-332, 2004.

[23] Condie, K.C. 2001. Mantle Plumes and Their Record in Earth History. Condie. Cambridge. University press, 306.

[24] DePaolo, D.J. 1981. Neodymium isotopes in the Colorado Front Range and crast-mantle evolution in the Proterozoic / Nature, 291, 21, 193-196.

[25] Dobretsov, N.L. 1997. Permian-Triassic magmatism and sedimentation in Eurasia as a reflection of a superplume. Doklady RAS. V. 354. N 2. P. 220-223.

[26] Dodin, D.A., Chernyshov, N.M., Cherednikova, O.I. 2001. Russian platinum-group element mineralogy. M., Geoinforμmark. 302 p.

[27] Dyuzhikov, O.A., Distler, V.V., Strunin, B.M., Mkrtshan, A.K., Sherman, M.L., Sluzenikin, S.F., Lurie, A.M. 1988. Geology and ore content of the Norilsk region. M., Nauka. 279 p.

[28] Ekimova, N.A., Serov, P.A., Bayanova, T.B., Elizarova, I.R., Mitrofanov, F.P. 2011. Distribution REE in sulfide minerals and Sm-Nd dating of processes ore forming layered basis intrusions. Doklady RAS. V. 436. N 1. P. 75-78.

[29] Ernst, R.E. & Buchan, K.L. 2003. Recognizing Mantle Plumes in the Geological Record. Annu. Rev. Earth Planet. Sci., 31, 469-523.

[30] Eules, H.V. & Cawthorn, R.G. 1995. The Bushveld Complex. Layered Intrusions. Developments in Petrology 15. Amsterdam; N.Y., Tokyo: Elsevier, 181-229.

[31] Faure, G.1986. Principles of Isotope Geology. 2 nd eds.Wiley. New York, 460.

[32] French, I.E., Heaman, L.M., Chacko, T., & Sristava, R.K. 2008. 1891-1883 Ma Southern Bastar –Cuddapah mafic igneous events, Judia: A newly recognized large igneous province. Precambrian Research, 160, 308-322.

[33] Goldstein, S.J. & Jacobsen, S.B. 1988. Nd and Sr isotopic systematics of river water suspended material implications for crystal evolution. Earth Plan. Sci. Letters, 87, 249-265.

[34] Gorbatschev, R. & Bogdanova, S. 1993. Frontiers in the Baltic Shield. Precambrian Research.V. 64, 3-21.

[35] Grachyov, A.F. 2003. Identification of mantle plumes on the basis of studying composition and isotope geochemistry of volcanic rocks. Petrology. V. 11. P. 618-654.

[36] Grochovskaya, T.L., Bakaed, G.F., Sholohnev, A.B., Lapina, M.I., Muravizkaya, G.H., Voitechovich, V.C. 2003. Ore platinometall mineralization in layered Monchegorsk magmatic complex (Kola peninsula, Russia) // Geology of ore deposited, 45, 4, 329-352.

[37] Groshev, N.Yu., Nitkina, Ye.A., Mitrofanov, F.P. 2009. Two-phase mechanism for the generation of PGE mafic rocks in the Fedorovo-Pana intrusion: New geological and isotope-geochemical data. Doklady RAS. V. 427. N 5. P. 669-673.

[38] Groves, D.I., Vielreicher, R.M., Goldfarb, R.J. 2005. Controls on the heterogeneous distribution of mineral deposits through time. Miner. Deposits and Earth Evolution, Geol. Soc. Sp. Publ. V. 248. P. 71-101.

[39] Hanski, E., Huhma, H., Smolkin, V. et al. 1990. The age of the ferropicric volcanics and comagmatic Ni-bearing intrusions at Pechenga, Kola Peninsula, USSR. Bull. Geol. Soc. Finland, 1990, V. 62, No 2, 123-133.

[40] Hanski, E., Walker, R.J., Huhma, H., & Suominen, I. 2001. The Os and Nd isotopic systematics of c. 2.44 Ga Akanvaara and Koitelainen mafic layered intrusions in northern Finland. Precambrian Research, 109, 73-102.

[41] Heaman, L.M. & LeCheminant, A.N. 1993. Paragenesis and U-Pb systematics of baddeleyite (ZrO). Chemical Geology. Elsevier, 110, 95-126.

[42] Heaman, L.M. 1997. Global mafic magmatism at 2.45 Ga: Remnants of an ancient large igneous province? Geology, 25, No 4, 299-302.

[43] Hofmann, A.W. 1997. Mantle geochemistry: the message from oceanic volcanism. Nature, 385, 219-229.

[44] Huhma, H., Clift, R.A., Perttunen, V. & Sakko, M. 1990. Sm-Nd and Pb isotopic study of mafic rocks associated with early Proterozoic continental rifting: The Perapohja schist belt in Northern Finland. Contrib. Mineral. Petrpol., 104, 369-379.

[45] Iljina, M., & Hanski, E. 2005. Layered mafic intrusions of the Tornio-Näränkävaara belt. In Lehtinen, M., Nurmi, P.A. & Rämo, O.T. (Eds.). Precambrian Geology of Finland – Key to the Evolution of the Fennoscandian Shield. Elsevier B.V., Amsterdam. 101-138.

[46] Irvine, T.N. 1982. Terminology for layered intrusions. Journal of Petrology. V. 23, P. 127-162.

[47] Jacobsen, S. B. & Wasserburg, G. J. 1984. Sm-Nd Isotopic Evolution of Chondrites and Achondrites, II. Earth Planet. Sci. Lett., 67, 137-150.

[48] Korchagin, A.U., Subbotin, V.V., Mitrofanov, F.P., Mineev, S.D. 2009. Kievey PGE-bearing deposit in the West Pana layered intrusion. In: Strategic mineral resources of Lapland, Apatity. P. 12-32.

[49] Kramm, U. 1993. Mantle components of carbonatites from the Kola Alkaline Province, Russia and Finland: A Nd-Sr study. Eur J. Mineral, 5, 985-989.

[50] Krogh, T.E. 1973. A Low-Contamination Method for Hydro-thermal Dissolution of Zircon and Extraction of U and Pb for Isotopic Age Determinations. Geochim. Cosmochim. Acta, 37, 485-494.

[51] Latypov, R.M., Mitrofanov, F.P., Alapieti, T.T., Halkoaho, A.A. 1999. Petrology of the Lower Layered Horizon, West Pana Tundra. Petrology. V. 7. N 5. P. 509-538.

[52] Latypov, R.M. & Chistyakova, S.Yu. 2000. Mechanism for differentiation of the Western-Pana layered intrusion. Apatity: Publ. of KSC RAS, 315.

[53] Li, C., Naldrett, A.J. 1993. Sulfide capacity of magma: a quantitative model and its applition to the formation of sulfide ores at Sudbury, Ontario. Economic Geology, 88, 1253-1260.

[54] Likhachyov, A.P. 2006. Platinum-copper-nickel and platinum deposits. M., Nauka. 496 p.

[55] Lubnina, N.V. 2009. East European craton from the Neoarchaean to the Palaeozoic in accordance with palaeomagnetic data. Thesis of a doctorate, M., 41 p.

[56] Ludwig, K.R. 1991. ISOPLOT - A plotting and regression program for radiogenic - isotope data, version 2.56 // Open-file report 91-445. US Geol. Surv., 40 p.

[57] Ludwig, K.R. 1999. ISOPLOT/Ex - A geochronological toolkit for Microsoft Excel, Version 2.05. Berkeley Geochronology Center Special Publication, 1a, 49.

[58] Ludwig, K.R. 1991. PBDAT - A Computer Program for Processing Pb-U-Th isotope Data. Version 1.22. Open-file report 88-542. US Geol. Surv., 38.

[59] Mints, M.V. 2011. Solid model for the deep structure of the Early Precambrian crust of the East European craton: Palaeogeodynamic consequences. Geotectonics. N 4. P. 3-29.

[60] Mitrofanov, F., Golubev, A. 2008. Russian Fennoscandia metallogeny. Abstr. To 33 IGC. Oslo, Norway.

[61] Mitrofanov, F.P. 2010. Metallogeny of the Kola-Karelian region, Baltic Shield. In: Fundamental geological problems of mineral deposits metallogeny. M., IGEM RAS. P. 257.

[62] Mitrofanov, F.P. 2005. New kinds of minerals resources in the Kola Province: Discoveries and perspectives. In Conference of V.I. Smirnov. M., IGEM RAS. P. 39-53.

[63] Mitrofanov, F.P., Malitch, K.N., Bayanova, T.B., Korchagin, A.U., Zhirov, D.V. Comparison of East-Scandinavian and Norilsk large plume mafic igneous provinces of PGE ores // Proceedings of the MSTU, 2012. V. 15. N 2. P. 380-394.

[64] Mitrofanov, F.P., Zhirov, D.V., Bayanova, T.B. Geological and isotope-geochemical forecast criteria of the PGM and/or Cu-Ni for mafic-ultramafic layered intrusions of the LIPs of Pre-Cambrian Shields // 34th International Geological Congress (IGC), 5-10 August 2012, Brisbane, Australia. SD-ROM–P3M-137 (P. 2300).

[65] Mitrofanov, F.P., Nerovich L.I. 2003. Time of igneous crystallization and metamorphic modifications in the Pyrshin and Abvar autonomous anorthosite intrusions of the Lapland granulite belt. Petrology. V. 11. N 4. P. 381-390.

[66] Mitrofanov, F.P, Smolkin, V.F., Bayanova, T.B, Neradovsky, Yu.N., Ohnenstetter, D., Ohnenstetter, M. & Ludden, J. 2002. Palaeoproterozoic (2.5-2.4 Ga) Plume Magmatism in the North-Eastern Baltic Shield and Origin of the PGE, Sulphide and Chromite Ore Deposit. Extended abstracts: 9th International Platinum Symposium. Billings, Montana, USA, 309-311.

[67] Mitrofanov, F.P. & Bayanova, T.B. 1999. Duration and timing of ore-bearing Palaeoproterozoic intrusions of Kola province. Mineral Deposits: Processes to Processing. Stanley et al. (Eds.). Balkema, Rotterdam, 1275-1278.

[68] Mitrofanov, F.P. & Nerovich, L.I. 2003. Timming of magmatic crystallization and metamorphic transformation in the Pyrshin and Abvar Autonomous anorthosite massifs, Lapland granulate belt. Petrology. V. 11, No 4, 343-351.

[69] Mitrofanov, F.P., Balabonin, N.L., Bayanova, T.B. et al. 1997. Main results from the study of the Kola PGE-bearing province, Russia. Mineral Deposits. Papunen (Eds.). Balkema, Rotterdam, 483-486.

[70] Mitrofanov, F.P., Balagansky, V.V., Balashov, Yu.A., Gannibal, L.F., Dokuchaeva, V.S., Nerovich, L.I., Radchenko, M.K. & Ryungenen, G.I. 1993. U-Pb age for gabbro-anorthosite of the Kola Peninsula. Doklady RAN, 331, 1, 95-98.

[71] Mitrofanov, F.P., Korchagin, A.U., Dudkin, K.O. & Rundkvist, T.V. 2005. Fedorovo-Pana layered mafic intrusion (Kola peninsula, Russia): Approaches, methods, and criteria for prospecting PGEs. Exploration for platinum-group elements deposits. Short Course delivered on behalf of the Mineralogical Association of Canada in Oulu, Finland, 35, 343-358.

[72] Naldrett, A.J. 2003. Igneous sulfide deposits of copper-nickel and PGE ores. SPb., SpbGU, 487 p.

[73] Nitkina, E.A. 2006. U–Pb Zircon Dating of Rocks of the Platiniferous Fedorova–Pana Layered Massif, Kola Peninsula. Doklady Earth Sciences, 408, 4, 551–554.

[74] Panteeva, S.V., Gladkochoub, D.P., Donskaya, T.V., Markova, V.V., Sandimirova, G.P. 2003. Determination of 24 trace elements in felsic rocks by inductively coupled plasma mass spectrometry after lithium metaborate fusion // Spectrochimica Acta Part B: Atomic Spectroscopy, 58, 2, 341-350.

[75] Papunen, H. and Gorbunov, G. I. (eds.). 1985. Nickel-Copper deposits of the Baltic Shield and Scandinavian Caledonides. Geological Survey of Finland, Bulletin 333, 394.

[76] Pirajno, F. 2007. Mantle plumes, associated intraplate tectono-magmatic processes and ore systems. Episodes, 30, 1, 6-19.

[77] Reischmann, T. 1995. Precise U-Pb age determination with baddeleyite (ZrO_2), a case study from the Phalaborwa Igneous Complex, South Africa. S. Afr. J. Geol., 1, 1-4.

[78] Richardson, S.H. & Shirey, S.B. 2008 Continental mantle signature of Bushveld magmas and coeval diamonds, Nature. 453, 910-913.

[79] Robb, L. 2008. Introduction to ore-forming processes. Blackwell Publ., 373 p.

[80] Scharer, U. & Gower, C.F. 1988. Crustal Evolution in Eastern Labrador: Constraints from Precise U-Pb Ages. Precambrian Research, 38, 405-421.

[81] Scharer, U., Wilmart, E., & Duchesne, J.-C. 1996. The Short Duration and Anorogenic Character of Anorthosite Magmatism: U-Pb Dating of the Rogaland Complex, Norway. Earth Planet. Sci. Lett., 139, 335-350.

[82] Schissel, D., Tsvetkov, A.A., Mitrofanov, F.P. & Korchagin, A.U. 2002. Basal Platinum-Group Element Mineralization in the Fedorov Pansky Layered Mafic Intrusion, Kola Peninsula Russia. Econ. Geol., 97, 1657-1677.

[83] Serov, P.A., Nitkina, E.A., Bayanova, T.B. & Mitrofanov, F.P. 2007. Comparison of the new data on dating using U-Pb and Sm-Nd isotope methods of early barren phase rocks and basal ore-hosting rocks of the Pt-bearing Fedorovo-Pansky layered intrusion (Kola peninsula). Doklady Earth Sciences, 415, 3, 1-3.

[84] Sharkov, Ye.V. 2006. Formation of layered intrusions and related mineralization. M., Scientific world, 364 p.

[85] Sharkov, E.V., Bogatikov, O.A., Grokhovskaya, T.L., Snyder, G.A., Taylor, L.A. 1995. Petrology and Ni-Cu-Cr-PGE mineralization of the largest mafic pluton in Europe: the early Proterozoic Burakovsky Layered Intrusion, Karelia, Rossia. International Geology Reviev, 37, 509-525.

[86] Skuf'in, P.K. & Bayanova, T.B. 2006. Early Proterozoic Central-Type Volcano in the Pechenga Structure and Its Relation to the Ore-Bearing Gabbro-Wehrlite Complex of the Kola Peninsula Petrology, 14, 6, 609-627.

[87] Sluzhenikin, S.F., Distler, V.V., Dyuzhikov, O.A., Kravzov, V.F., Kunilov, V.T., Laputina, N.P., Turovzev, D.M. 1994. Low-sulfide PGE mineralization in the Norilsk differentiated intrusions. Geology of ore deposits. V. 36. N 3. P. 195-217.

[88] Smolkin, V.F., Kremenetsky, A.A., Vetrin, V.R. 2009. Geological and geochemical model of the Palaeoproterozoic ore-magmatic systems, Baltic Shield. National Geology, Iss. 3. P. 54-62.

[89] Smolkin, V.F., Fedotov, Zh.A, Neradovsky, Yu.N., Bayanova, T.B. et al. 2004. Layered intrusions of the Monchegorsk ore region: petrology, mineralization, isotope features and deep structure. Mitrofanov, F.P. & Smolkin, V.F. (Eds.). Part 1. Apatity: publ. by Kola Science Centre RAS, 177 p.

[90] Stacey, J. S. & Kramers, J. D. 1975. Approximation of Terrestrial Lead Isotope Evolution by a Two-Stage Model. Earth Planet. Sci. Lett., 26, 207-221.

[91] Starostin, V.I., Sorokhtin, O.G. 2010. Recycling origin model for sulfide copper-nickel deposits with PGEs of Norilsk type. Proceedings of the Earth Sciences Division, RANS, Iss. 19. P. 5-10.

[92] Steiger, R.H. & Jager, E. 1977. Subcoμmission on Geo-chronology: Convention on the Use of Decay Constants in Geo- and Cosmochronology. Earth Planet. Sci. Lett., 36, 359-362.

[93] Tolstikhin, I.N. & Marty, B. 1998. The evolution of terrestrial volatiles: A view from helium, neon, argon and nitrogen isotope modeling. Chemical Geology, 147, 27-52.

[94] Tolstikhin, I.N., Dokuchaeva, V.S., Kamensky, I.L. & Amelin, Yu.V. 1992. Juvenile helium in ancient rocks: II. U-He, K-Ar, Sm-Nd, and Rb-Sr systematics in the Monchepluton. $^{3}He/^{4}He$ rations frozen in uranium-free ultramafic rocks. Geochim. Cosmochim. Acta, 56, 987-999.

[95] Tuganova, Ye.V. 2000. Formational types, genesis, and emplacement mechanisms for sulfide platinum-copper-nickel and platinum deposits. VSEGEI, 102 p.

[96] Verba, M.L., Vinogradov, A.N., Mitrofanov, F.P. 2005. Evolution of the Earth crust and mineragenic potential of the Barents region. Structure of the lithosphere in the Russian part of the Barents region. Petrozavodsk, Karelian Science Centre RAS. P. 256-311.

[97] Vogel, D.C., Vuollo, J.I., Alapieti, T.T. & James, R.S. 1998. Tectonic, stratigraphic, and geochemical comparison between ca. 2500-2440 Ma mafic igneous events in the Canadian and Fennoscandian Shields. Precambrian Research, 92, 89-116.

[98] Vrevsky, A.B. & Levchenkov, O.A. 1992. Geological-geochronological scale of the endogenous processes operated within the Precambrian complexes of the central part of the Kola Peninsula. In: Mitrofanov, F.P. & Bolotov, V.I. (Eds.). Geodynamics and deep structure of the Soviet Baltic Schield. Apatity, 150 p.

[99] Vuollo, J.I. & Huhma, H. 2005. Palaeoproterozoic mafic dykes in NE Finland. In: Lehtinen, M., Nurmi, P.A. & Rämö, O.T. (eds.) Precambrian Geology of Finland. Elsevier. B.V. Amsterdam, 195-236.

[100] Vuollo, J.I., Huhma, H., Stepana, V. & Fedotov, Zh.A. 2002. Geochemistry and Sm-Nd isotope studies of a 2.45 Ga dyke swarm: hints at parental magma compositions and PGE potential to Fennoscandian layered intrusions. In: Boudreau, A. (ed.). 9th Intern. Platinum Symp., 21-25 July, 2002, Billings, Montana USA, 469-470.

[101] Yekimova, N.A., Serov, P.A., Bayanova, T.B., Yelizarova, I.R., Mitrofanov, F.P. 2011. The REE distribution in sulphide minerals and Sm-Nd age determination for the ore-forming processes in mafic layered intrusions // Doklady RAS, 436, 1, 75-78.

[102] Yi-Gang, Xu. 2007. Mantle plume, large igneous provinces and lithospheric evolution. Episodes. V. 30. No 1, P. 5.

[103] Zhuravlyov, A.Z., Zhuravlyov, D.Z., Kostitsyn, Yu.A., Chernyshov, I.V. 1987. Determination of the Sm-Nd ration for geochronological purposes // Geochemistry, 8, 1115-1129.

[104] Zozulya, D.R., Bayanova, T.B. & Nelson, E.G. 2005. Geology and Age of the Late Archaean Keivy Alkaline Province, Northeastern Baltic Shield. Geology, 113, 601-608.